Fate of PFAS and Other Contaminants During Leachate Evaporation

October 2023

Youneng Tang
FAMU-FSU College of Engineering
Department of Civil and Environmental Engineering

Mojtaba Nouri Goukeh
FAMU-FSU College of Engineering
Department of Civil and Environmental Engineering

PROJECT TITLE: Fate of PFAS and Other Contaminants During Leachate Evaporation

PRINCIPAL INVESTIGATOR: Youneng Tang, Ph.D., Associate Professor
Department of Civil and Environmental Engineering, FAMU-FSU College of Engineering
2525 Pottsdamer Street Suite A132 Tallahassee FL 32310; Tel: 850-4106119;
ytang@eng.famu.fsu.edu

PROJECT WEBSITE: https://web1.eng.famu.fsu.edu/~ytang/leachate_evaporation.html

PROJECT DURATION: October 1st, 2022 to September 30st, 2023

ABSTRACT:
Landfilling is one of the most commonly used waste disposal methods because it is a relatively cost-effective and controlled process for transforming waste into stabilized materials. However, the generation of leachate remains an inevitable consequence of landfilling. Landfill leachate contains various contaminants such as heavy metals, ammonia, salts, and organic contaminants (e.g., pesticides, chlorinated aliphatics, per- and polyfluoroalkyl substances (PFAS)). Leachate evaporation is one of the methods for leachate management, but knowledge about fate of contaminants during leachate evaporation in the literature focuses on some conventional contaminants in the condensate. The objective of this project is to expand knowledge in the area of fate of contaminants during leachate evaporation by answering three questions: 1) What happens to PFAS and other contaminants when the leachate is evaporated? 2) What are the distribution ratios of PFAS? 3) What is the effect of reintroduction of the concentrated leachate residual into the landfill?

We used a rotary evaporator to evaporate landfill leachate sampled from three landfills in Florida. We took samples from the leachate residuals and condensates at 0%, 12.5%, 25%, 50%, 75%, and 90% of evaporation. We observed three different patterns for contaminants in leachate residuals during evaporation. Regarding the first pattern, the concentrations of total dissolved solids (TDS), total suspended solids (TSS), chemical oxygen demand (COD), total organic carbon (TOC), five-day biochemical oxygen demand (BOD_5), zinc, chromium, and PFAS measured by liquid chromatography with tandem mass spectrometry (LC/MS/MS) increased in all three leachate residuals during evaporation. Regarding the second pattern, the concentrations of ammonia, naphthalene, p-cresol, pyridine, and fluorotelomer alcohols (FTOHs) decreased in all three leachate residuals during evaporation since they are all volatile compounds. Regarding the third pattern, the change of pH, aniline, and phenol in the residuals depended on the leachate as they could be produced as reaction products. Their change in the condensates were different from the residuals. The concentrations of TDS, TOC, BOD_5, pyridine, FTOHs, and naphthalene kept decreasing in the condensates due to dilution and/or further transfer to the gas phase. TSS, zinc, chromium, and the PFAS measured by LC/MS/MS remained below their detection limits in the condensates. The change pattern of pH, aniline, and phenol in the condensates still depended on the leachate.

To further study the distribution of PFAS, we spiked a synthetic leachate with four FTOHs and seven perfluoroalkyl carboxylic acids (PFCAs, C4-C10), respectively, at 500 µg/L for each PFAS. At 90% of evaporation, more than 99.9% of each FTOH in mass were removed from the system (i.e., leachate residual and condensate), with FTOHs below the detection limits in the residual and <0.2% (in mass) in the condensates. A range of 112-133% (in mass) of PFCAs with the exception of PFDA remained in the leachate residual, with 0.138-6.83% (in mass) transferred to the condensate, and -12.3 – -39.8% being produced due to reactions. More than 100% recovery in the residual was potentially due to conversion from PFCA precursors during heating. We also found that the percentages of PFCAs (in mass) in condensate increased with the increase of the PFCA chain length, probably due to the lower solubility of longer-chain PFACs.

We mixed leachate #1 with its concentrated residual corresponding to 90% evaporation at a volume ratio of 9:1, and then compared this mixture with leachate #1 for the fate of contaminants during evaporation. Adding concentrated leachate residual significantly increased the concentration of non-volatile compounds in the residual such as TDS and TSS, but slightly decreased the concentrations of volatile compounds such as ammonia, naphthalene, p-cresol, pyridine, and FTOHs because of dilution.

METRICS REPORTING

Student Researchers:

Last name, first name	Email	Anticipated degree	Department
Mojtaba Nouri Goukeh	Mn20f@my.fsu.edu	Ph.D.	Civil and Environmental Engineering

Metrics:

1. List research publications resulting from THIS Hinkley Center project.

We are preparing a manuscript to be submitted to a journal for publication. The tentative title is "Fate of contaminants during leachate evaporation".

2. List research presentations resulting from (or about) THIS Hinkley Center project.

None.

3. List who has referenced or cited your publications from this project.

None.

4. How have the research results from THIS Hinkley Center project been leveraged to secure additional research funding? What additional sources of funding are you seeking or have you sought?

We have submitted a proposal regarding volatile PFAS to the Department of Defense.

5. What new collaborations were initiated based on THIS Hinkley Center project?

None.

6. How have the results from THIS Hinkley Center funded project been used (not will be used) by the FDEP or other stakeholders?

Florida Department of Environmental Protection (FDEP) personnel have commented that they reviewed information from this project in order to keep the FDEP PFAS Dynamic Plan as current as possible. Past research papers are listed in The Hinkley Center for Solid and Hazardous Waste

Management section of the Dynamic Plan. It is expected, based on FDEP involvement with this project that this paper will be included in the upcoming revision to the Dynamic Plan.

ACKNOWLEDGEMENTS

Technical Advisory Group (TAG)

Name & title	Affiliation
Mr. Bruce Marvin, P.E.	Geosyntec Consultants
Mr. Chao Zhou, P.E.	Geosyntec Consultants
Ms. Claudia Mack, P.E.	Geosyntec Consultants
Mr. Kevin Warner, P.E.	Geosyntec Consultants
Mr. Terry Johnson	Waste Management Inc.
Mr. Sterling Carroll, P.E.	Florida Rural Water Association
Dr. Owete S. Owete, P.E.	WSP USA
Mr. Joseph Dertien, P.E.	Florida Department of Environmental Protection
Dr. Kerry Tate	Florida Department of Environmental Protection
Ms. Lauren J. Coleman, P.E.	Florida Department of Environmental Protection
Ms. Shanin Speas-Frost, P.E.	Florida Department of Environmental Protection
Ms. Walsta Jean-Baptiste, P.G.	Florida Department of Environmental Protection

TABLE OF CONTENTS

LIST OF TABLES

LIST OF FIGURES

LIST OF ABBREVIATIONS AND ACRONYMS

ADONA	4,8-dioxa-3Hperfluorononanoic acid
AEL SOP	Advanced Environmental Laboratories Standard Operation Procedure
BDL	Below detection limit
BOD	Biochemical oxygen demand
BOD_5	Five-day biochemical oxygen demand
CAR/PDMS	Carboxen/Polydimethylsiloxane
CFR	Code of Federal Regulations
COD	Chemical oxygen demand
DOC	Dissolved organic carbon
EC	Electric conductivity
EPA	Environmental protection agency
FTOHs	Fluorotelomer alcohol
GC/MS	Gas chromatography-mass spectrometry
HFPO-DA	Hexafluoropropylene oxide dimer acid
LC/MS/MS	Liquid chromatography with tandem mass spectrometry
MP-AES	Microwave plasma-atomic emission system
N.A.	Not available
NFDHA	Nonafluoro-3,6-dioxaheptanoic acid
PFAS	Per- and polyfluoroalkyl substances
PFBA	Perfluorobutanoic acid
PFBS	Perfluorobutane sulfonic acid
PFCAs	Perfluoroalkyl carboxylic acids
PFDA	Perfluorodecanoic acid
PFDoA	Perfluorododecanoic acid
PFEESA	Perfluoro (2-ethoxyethane) sulfonic acid
PFHpA	Perfluoroheptanoic acid
PFHpS	Perfluoroheptane sulfonic acid
PFHxA	Perfluorohexanoic acid
PFHxS	Perfluorohexane sulfonicacid
PFMBA	Perfluoro-3-methoxypropanoic acid
PFMPA	Perfluoro-4-methoxybutanoic acid
PFNA	Perfluorononanoic acid
PFOA	Perfluorooctanoic acid
PFOS	Perfluorooctane sulfonic acid
PFPeA	Perfluoropentanoic acid
PFPeS	Perfluoropentane sulfonic acid
PFUnA	Perfluoroundecanoic acid
SPME	Solid phase microextraction
TDS	Total dissolved solids
TOC	Total organic carbon
TSS	Total suspended solids
4:2 FTOH	4:2 Fluorotelomer alcohol

4:2 FTS	4:2 Fluorotelomer sulfonic acid
6:2 FTOH	6:2 Fluorotelomer alcohol
6:2 FTS	6:2 Fluorotelomer sulfonic acid
8:2 FTOH	8:2 Fluorotelomer alcohol
8:2 FTS	8:2 Fluorotelomer sulfonic acid
9Cl-PF3ONS	9-Chlorohexadecafluoro-3-oxanonane-1-sulfonic acid
10:2 FTOH	10:2 Fluorotelomer alcohol
11Cl-PF3OUdS	11-Chloroeicosafluoro-3-oxaundecane-1-sulfonic acid

EXECUTIVE SUMMARY

Introduction

Landfilling is widely used for waste disposal, since it offers a cost-effective and controlled process that degrades waste into stabilized materials. Compared to alternatives such as incineration and composting, landfilling remains the most commonly used waste disposal method. Modern landfills are designed with advanced engineering techniques to minimize the environmental impacts associated with municipal solid waste. However, the generation of leachate remains an unavoidable consequence of landfilling. Landfill leachate contains various contaminants such as heavy metals, ammonia, salts, and organic contaminants (e.g., pesticides, chlorinated aliphatics, per- and polyfluoroalkyl substances (PFAS)).

Several technologies have been used for the treatment of landfill leachate, including biological technologies such as activated sludge and fluidized bed reactor, chemical technologies such as the Fenton process and chemical precipitation, as well as physical-chemical technologies like adsorption and membrane separation. In recent years, evaporation has gained attention for to its usefulness in treating leachate with pollutants at high concentrations.

Evaporation is a process in which substances transition from a liquid form to a gaseous state. Condensate can be generated, which is usually of higher water quality and more easily manageable for disposal compared to the influent. Additionally, the volume of concentrated residuals resulting from the evaporation process is significantly smaller compared to the original volume of the leachate. Although more and more landfills are using evaporators for leachate management, knowledge about the fate of contaminants during evaporation has focused on the conventional contaminants in the condensate.

The overarching goal of this project is to expand knowledge of the fate of more contaminants during leachate evaporation including certain PFAS and other federally regulated contaminants. To achieve the this objective, the following three tasks were completed:

> Task 1: effects of leachate evaporation on the fate of PFAS and contaminants regulated by 40 CFR 445.11
> Task 2: distribution ratios of PFAS (PFAS in residual: PFAS in condensate: other PFAS)
> Task 3: effects of reintroduction of the concentrated leachate residuals.

Methods

In Task 1, we used a rotary evaporator to evaporate three landfill leachates sampled from three landfills, respectively, in Florida. For each landfill, 1.6 liters of leachate was evaporated at a temperature of 77 °C via a water bath and a vacuum pressure of -650 mmHg (relative to the atmospheric pressure of 0). We took samples from the leachate residuals and condensates when 0%, 12.5%, 25%, 50%, 75%, and 90% evaporation was completed.

We measured total dissolved solids (TDS), total suspended solids (TSS), pH, total organic carbon (TOC), chemical oxygen demand (COD), five-day biochemical oxygen demand (BOD$_5$), ammonia, α-terpineol, aniline, benzoic acid, naphthalene, p-cresol, phenol, pyridine, arsenic, chromium, zinc, and PFAS in the leachate residuals and condensates. These contaminants were classified in five groups, including 1) general physical parameters, 2) general chemical parameters, 3) metals, 4) organic contaminants, and 5) PFAS.

Task 2 was an extension of Task 1 but focused on PFAS. In Task 2, we used synthetic leachate that contained 1,000 mg/L of humic acid and 1,500 mg/L of NH$_4$Cl. We first spiked the synthetic leachate with 4:2 fluorotelomer alcohol (4:2 FTOH), 6:2 fluorotelomer alcohol (6:2 FTOH), 8:2 fluorotelomer alcohol (8:2 FTOH), and 10:2 fluorotelomer alcohol (10:2 FTOH) at 500 µg/L for each FTOH. We evaporated the synthetic leachate and took samples from the leachate residual and condensate when 1.5%, 3%, 6%, 12.5%, 25%, 50%, 75%, and 90% evaporation was completed. To evaluate the fate of perfluoroalkyl carboxylic acids (PFCAs) during leachate evaporation, we spiked the same synthetic leachate with perfluorodecanoic acid (PFDA, C10), perfluorononanoic acid (PFNA, C9), perfluorooctanoic acid (PFOA, C8), perfluoroheptanoic acid (PFHpA, C7), PFHxA perfluorohexanoic acid (PFHpA, C6), perfluoropentanoic acid (PFPeA, C5), and Perfluorobutanoic acid (PFBA, C4) at 500 µg/L for each PFCA. We evaporated the synthetic leachate and took samples from the leachate residual and condensate when 0% and 90% evaporation was completed. The FTOHs were measured using gas chromatography - mass spectrometry (GC/MS) and the PFCAs were measured using liquid chromatography with tandem mass spectrometry (LC/MS/MS).

Task 3 was similar to Task 1 except the following major difference. While three raw leachates were used in Task 1, leachate #1 was selected and used in Task 3. We mixed 1,440 mL of leachate #1 with 160 mL of leachate residual #1 corresponding to 90% of evaporation, and then evaporated the mixture.

Results and Discussion
We observed three patterns for contaminants in leachate residuals during evaporation. Regarding the first pattern, the concentrations of TDS, TSS, COD, TOC, BOD$_5$, zinc, chromium, and PFAS measured by LC/MS/MS increased in all three leachate residuals during evaporation. Regarding the second pattern, the concentrations of ammonia, naphthalene, p-cresol, pyridine, and fluorotelomer alcohols (FTOHs) decreased in all three leachate residuals during evaporation since they are volatile compounds. Regarding the third pattern, the change of pH, aniline, and phenol in the residuals depended on the leachate as they could be produced as reaction products. Their change in the condensates were different from the residuals. The concentrations of TDS, TOC, COD, BOD$_5$, pyridine, FTOHs, and naphthalene kept decreasing in the condensates due to dilution and/or further transfer to the gas phase. TSS, zinc, chromium, and the PFAS measured by LC/MS/MS remained below their detection limits in the condensates. The change pattern of pH, aniline, and phenol in the condensates still depended on the leachate.

To further evaluate the fate of PFAS during leachate evaporation, we spiked the synthetic leachate with FTOHs and PFCAs at 500 µg/L for each PFAS. At 90% of evaporation, more than 99.9% of each FTOH in mass were removed from the system (i.e., leachate residual and condensate), with

FTOHs below the detection limits in the residual and less than 0.2% (in mass) in the condensate. The concentrations of PFCAs in the leachate residual increased by 7.8 to 12 times at 90% evaporation, suggesting that they accumulated during the evaporation. Regarding distribution, 112-133% (in mass) of PFCAs except perfluorodecanoic acid (PFDA) stayed in the leachate residual, 0.138-6.83% (in mass) were transferred to the condensate, and -12.3 – -39.8% being produced due to reactions. More than 100% recovery in the residual was probably due to conversion from PFCA precursors during heating. We also found that the percentages of PFCAs in mass in the condensate increased with the increase of PFCA chain length, probably due to lower solubility of longer-chain PFACs.

We mixed leachate #1 with its concentrated residual corresponding to 90% evaporation at a volume ratio of 9:1 to evaluate the effects of reintroduction of the concentrated leachate residual. Adding the concentrated leachate residual significantly increased the concentrations of non-volatile compounds in the residual. For example, adding just 10% concentrated leachate residual at least doubled the TDS and TSS in the residual at 90% evaporation. On the other hand, for volatile compounds such as ammonia, naphthalene, p-cresol, pyridine, and FTOHs, the reintroduction of residual slightly decreased their concentrations in the residual at 90% evaporation because of dilution by the concentrated leachate that contained no or negligible volatile compounds.

1. INTRODUCTION

1.1. Background

The increase in population, consumer-driven lifestyles, and the expansion of industrial activities contribute significantly to a visible rise in the generation of municipal solid waste (Bakhshoodeh et al., 2020). Landfilling is a widely employed method for waste disposal, as it offers a cost-effective and controlled process for degrading waste into stabilized materials. Compared to alternatives such as incineration and composting, landfilling remains the most commonly utilized approach. Modern landfills are meticulously designed with advanced engineering techniques to minimize the environmental impacts associated with municipal solid waste. However, the generation of leachate remains an unavoidable consequence of landfilling (Wiszniowski et al., 2006).

Landfill leachate is a combination of rainwater that has seeped through the landfill, water generated from the biodegradation of waste, and the moisture present within the waste itself. It contains a lot of heavy metals, ammonia, salts, and organic contaminants (e.g., pesticides, chlorinated aliphatics, per- and polyfluoroalkyl substances (PFAS)) (Liu et al., 2015; Babaei et al., 2021; Teng et al., 2021). Landfill leachate has been identified as toxic, posing potential dangers to the nearby environment and ecosystems (Baderna et al., 2019). By infiltration of landfill leachate into the soil, both surface and groundwater resources could be contaminated (Cheng et al., 2021). The quality of landfill leachate is influenced by several factors, including the age of the landfill, precipitation level, seasonal weather variation, waste type, and composition. These factors can vary depending on the standard of living of the surrounding population and the structure of the landfill site. Among the mentioned factors, age of the landfill usually played the key role (Renou et al., 2008). As landfills age, the ratio of biochemical oxygen demand (BOD) to chemical oxygen demand (COD) in the leachate tends to decrease. Initially, the ratio can be around 0.70, but over time, it can decrease to 0.04 (Chian et al., 1976). The decrease in the BOD/COD ratio in aged landfill leachate is attributed to the release of recalcitrant organic molecules from the solid waste materials and the reaction of the degradable organic molecules. As a result, older landfill leachate is characterized by a low BOD/COD ratio and relatively high levels of ammonia nitrogen (Renou et al., 2008). Regulatory standards for landfill leachate vary from country to country. In the United States, the Code of Federal Regulations (CFR) plays a significant role in setting standards for environmental protection.

Title 40 of CFR contains regulations pertaining to environmental protection. Section 40 CFR 445.11 refers to regulations related to landfill leachate. Specifically, Section 40 CFR 445.11 contains the limitations and standards for pollutants that can be present in landfill leachate. These pollutants include heavy metals, organic compounds, and general leachate parameters such as BOD, COD, and pH. Table 1 shows effluent limitations based on 40 CFR 445.11 (ECFR, 2023).

Table 1. Effluent limitations for contaminants regulated by Title 40 of Code of Federal Regulations (CFR) 445.11

Regulated parameter	Units	Maximum daily	Maximum monthly average
TSS[1]	mg/L	88	27
pH	-	6-9	6-9
Ammonia	mg/L	10	4.9
BOD$_5$[2]	mg/L	220	56
Zinc	mg/L	0.535	0.296
Arsenic	mg/L	1.1	0.54
Chromium	mg/L	1.1	0.46
α-Terpineol	mg/L	0.042	0.019
Aniline	mg/L	0.024	0.015
Benzoic acid	mg/L	0.119	0.073
Naphthalene	mg/L	0.059	0.022
p-Cresol	mg/L	0.024	0.015
Phenol	mg/L	0.048	0.029
Pyridine	mg/L	0.072	0.025

Notes:
[1] TSS = Total suspended solids
[2] BOD$_5$ = Five-day biochemical oxygen demand

1.2. Leachate treatment processes

Several technologies have been developed for the treatment of landfill leachate, including biological treatment processes like activated sludge and fluidized bed reactor processes, chemical treatment processes such as the Fenton process and chemical precipitation, as well as physical-chemical treatment processes like adsorption and membrane separation. These technologies offer different approaches to effectively treat landfill leachate (Teng et al., 2021). Some methods of leachate management are introduced below.

Leachate transfer: A common approach to treating landfill leachate is to combine it with municipal sewage and treat them together in the municipal wastewater treatment plant. The practice of treating landfill leachate together with municipal sewage has faced growing scrutiny. This is because landfill leachate contains organic inhibitory compounds with low biodegradability and heavy metals, which can adversely impact the treatment efficiency of the municipal sewage treatment plant. Additionally, these substances may lead to increased concentrations of pollutants in the effluent, raising environmental concerns and challenging the overall effectiveness of the treatment process (Çeçen et al., 2004). Therefore, alternative treatment methods have been sought to address the unique challenges posed by landfill leachate.

Leachate recirculation: Leachate recirculation is an inexpensive technique that involves the process of returning moisture derived from an active or closed landfill site back into the landfill (Schiopu et al., 2010). It decreases the stabilization time of landfill leachate because of higher moisture content and faster decomposition of waste materials (Reinhart et Al., 1996). Also, it increases the methane production rate (Sanphoti et al., 2006). Merely relying on recirculation alone may be insufficient to decrease the amount of leachate and enable its direct discharge into municipal wastewater treatment facilities (Schiopu et al., 2010).

Biological treatment: Various aerobic and anaerobic processes have been used for the leachate management. These processes include suspended-growth biomass processes and attached-growth biomass systems. Suspended-growth biomass processes include activated sludge processes, lagoons, and sequencing batch reactors. Attached-growth biomass systems include trickling filters, moving-bed biofilm reactor (Renou et al., 2008). One limitation of biological processes is that they are not effective for non-biodegradable contaminants.

Physical-chemical processes: These processes have a better performance for the removal of non-biodegradable compounds. These processes include flotation, coagulation-flocculation, chemical precipitation, adsorption, chemical oxidation, and membrane separation (Wiszniowski et al., 2006; Renou et al., 2008).

Evaporation: Evaporation can be described as a process in which a substance transitions from a liquid form to a gaseous state (Rehman., 2004). Condensate can be generated, which is of higher quality and more easily manageable for disposal compared to the raw leachate. Additionally, the volume of concentrated residuals resulting from the evaporation process is significantly smaller compared to the original volume of leachate (Birchler et al., 1994).

The use of evaporation technology in leachate treatment has garnered attention due to its ability for treating leachate with high concentrations of pollutants (Liang et al., 2013; Zhou et al., 2014). Low-temperature vacuum evaporation is a method that heats and evaporates leachate in a temperature lower than the boiling point of water (Zhang et al., 2022). This technology produces high quality condensate that contains much less contaminants compared to influent. Also, this technology reduces the volume of the leachate by up to 90-95% (Keyikoglu et al., 2021).

Fate of contaminants in the leachate evaporators

Although more and more landfills are using evaporators for leachate management, there is limited knowledge about the fate of contaminants during the leachate evaporation. As shown in Table 2, most studies have focused on the general parameters such as COD, dissolved organic carbon (DOC), NH_3, and total Kjeldahl nitrogen (TKN). Also, most of these studies only evaluated the quality of the condensate and did not evaluate the quality of the leachate residual.

Table 2. Previous studies that evaluated the fate of contaminants during leachate evaporation

Study	Matrix	Evaporation method	Operation conditions	Removal percentage in condensate[9] (%)	Removal percentage in residual leachate[10] (%)
Zhang et al., 2022	Landfill leachate	Rotary evaporator	$T^1 = 60\ °C$ $P^2 = 85$ mmHg	$COD^3 = 98.7$ $DOC^4 = 92.6$ $NH_4^+ = 84.3$	N.A.[8]
Sprovieri et al., 2020	Landfill leachate	Heating plate	$T = 300\ °C$ $P = 535$ mmHg	$NH_4^+ = 6$	$NH_4^+ = 100$
Afsharnia et al., 2012	Landfill leachate	Water bath	$T = 100\ °C$ $P = 760$ mmHg	$COD = 88$ $TKN^5 = 90$ $EC^6 = 92$ $Ni = 97$ $Zn = 96$	N.A.
Palma et al., 2002	Landfill leachate	Rotary evaporator	$T = 40\ °C$ $P = 20 - 400$ mmHg	$COD = 99$ $TOC^7 = 99$ $NH_4^+ = 85$ $Pb^{2+} = 100$ $Fe^{3+} = 100$ $Ca^{2+} = 100$ $K^+ = 100$ $Na^+ = 100$	$COD = -292$ $TOC = -293$ $NH_4^+ = -263$ $Pb^{2+} = -300$ $Fe^{3+} = -2261$ $Ca^{2+} = -5270$ $K^+ = -205$ $Na^+ = -471$
Bouchareb et al., 2022	Landfill leachate	Rotary evaporator	$T = 70 - 90\ °C$ $P = 60$ mmHg	$COD = 99.9$ Total phenol = 95 $NH_4^+ = 83$ $EC = 88$	N.A.

Notes:
[1] T = Temperature; [2] P = Pressure; [3] COD = Chemical oxygen demand; [4] DOC = Dissolved organic carbon; [5] TKN = Total Kjeldahl nitrogen; [6] EC = Electric conductivity; [7] TOC = Total organic carbon; [8] N.A. = Not available.
[9] Removal percentage in condensate was calculated by (concentration in residual at 0% evaporation - concentration in condensate at 90% evaporation)/ concentration in residual at 0% evaporation.
[10] Removal percentage in leachate residual was calculated by (concentration in residual at 0% evaporation - concentration in residual at 90% evaporation)/ concentration in residual at 0% evaporation.

1.3. Project objectives and tasks

The overarching goal of this project is to expand knowledge in the area of fate of contaminants during the evaporation of landfill leachate. The objectives of this project are to answer the following questions:

1) What happens to PFAS and other contaminants when the leachate is evaporated? Do they concentrate within the residual? Are they emitted into the atmosphere?
2) What affects the distribution ratios of PFAS -- PFAS in residual: PFAS in condensate: PFAS in gas?
3) What are the effects of the reintroduction of the concentrated leachate residuals on the chemical concentrations of future leachate?

To achieve the three objectives, three tasks are to be completed, including:

Task 1: effects of leachate evaporation on the fate of PFAS and contaminants regulated by 40 CFR 445.11

Task 2: distribution ratios of PFAS = PFAS in residual: PFAS in condensate: PFAS in gas

Task 3: effects of reintroduction of the concentrated leachate residuals

2. METHODS

2.1. Effects of leachate evaporation on the fate of PFAS and contaminants regulated by 40 CFR 445.11 (Task 1)

2.1.1 Leachate evaporation

We used a rotary evaporator (see Figure 1) to evaporate landfill leachate sampled from three landfills in Florida. For each landfill, 1.6 liters of leachate was evaporated at a temperature of 77 °C via a water bath and a vacuum pressure of -650 mmHg (relative to the atmospheric pressure of 0). We took samples from the leachate residual and condensate when 0%, 12.5%, 25%, 50%, 75%, and 90% evaporation was completed.

Figure 1. Lab-scale evaporator

We measured 14 contaminants regulated by 40 CFR 445.11, total dissolved solids (TDS), TOC, COD, and PFAS. The 14 contaminants regulated by 40 CFR 445.11 include five-day biochemical oxygen demand (BOD$_5$), total suspended solids (TSS), ammonia, α-terpineol, aniline, benzoic acid, naphthalene, p-cresol, phenol, pyridine, arsenic, chromium, zinc, and pH. These contaminants have been classified in five groups, including 1) general physical parameters, 2) general chemical parameters, 3) metals, 4) organic contaminants, and 5) PFAS.
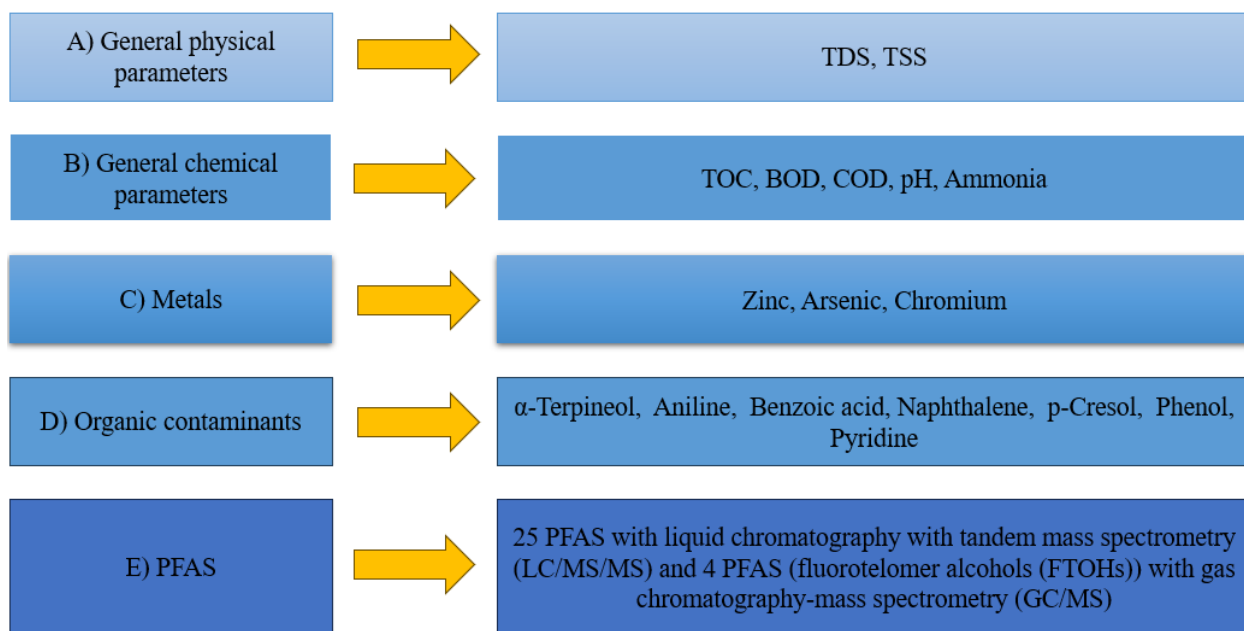
Figure 2. Parameters measured in landfill leachate

2.2. Distribution ratios of PFAS (Task 2)

Task 2 extended on Task 1, but focused on PFAS in synthetic leachate. The synthetic leachate contained 1,000 mg/L of humic acid and 1,500 mg/L of NH_4Cl (Ferraz et al., 2020a; Ferraz et al., 2020b). We spiked the synthetic leachate with 4:2 fluorotelomer alcohol (4:2 FTOH), 6:2 fluorotelomer alcohol (6:2 FTOH), and 8:2 fluorotelomer alcohol (8:2 FTOH), and 10:2 fluorotelomer alcohol (10:2 FTOH) at 500 µg/L for each FTOH. We evaporated the synthetic leachate and took a sample from the leachate residual and a sample from the condensate when 1.5%, 3%, 6%, 12.5%, 25%, 50%, 75%, and 90% evaporation was completed.

To observe the fate of perfluoroalkyl carboxylic acids (PFCAs) during leachate evaporation, we then spiked the synthetic leachate with perfluorodecanoic acid (PFDA, C10), perfluorononanoic acid (PFNA, C9), perfluorooctanoic acid (PFOA, C8), perfluoroheptanoic acid (PFHpA, C7), PFHxA perfluorohexanoic acid (PFHpA, C6), perfluoropentanoic acid (PFPeA, C5), and Perfluorobutanoic acid (PFBA, C4) at 500 µg/L for each PFCA. We took samples from the leachate residual and the condensate when 0% and 90% evaporation was completed. The samples were measured in a commercial lab by liquid chromatography with tandem mass spectrometry (LC/MS/MS). We also did the same experiment without adding PFCAs as a control.

Finally, we calculated the distribution ratios of PFAS when 90% of evaporation was achieved. The ratios were PFAS in residual (mass): PFAS in condensate (mass): other PFAS (mass). Other PFAS was calculated as the initial PFAS in leachate (mass) - PFAS in residual (mass) - PFAS in condensate (mass).

2.3. Effects of reintroduction of the concentrated leachate residuals (Task 3)

This task was similar to Task 1 except for the following major difference. While three raw leachates were used in Task 1, leachate #1 was selected and used in Task 3. As shown in Figure 3, 1,440 mL of leachate #1 was mixed with 160 mL of leachate residual #1 (corresponding to 90% of evaporation) and then tested as in Task 1.
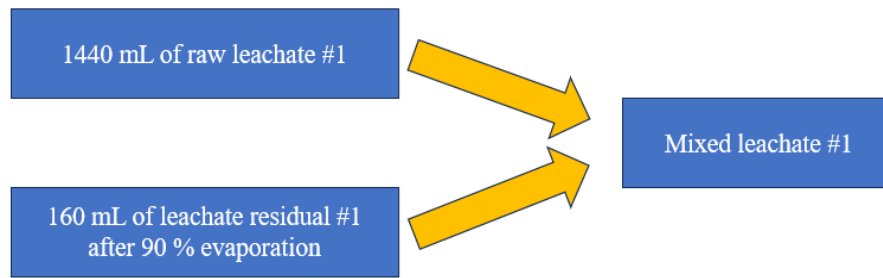
Figure 3. Making mixed leachate by the combination of raw leachate and leachate residual

2.4. Chemical analysis

Table 3 shows the list of leachate parameters and the summary of methods that we used for the measurements. Each parameter is briefly discussed as follows:

TOC: TOC was measured by a total organic carbon analyzer (Shimadzu TOC-VCSH) based on combustion catalytic oxidation in a commercial laboratory (Li et al., 2019).

COD: We measured COD by HACH Method 800 via a HACH spectrophotometer (DR3900) (Elnakar and Buchanan, 2020). Samples were diluted, when necessary, using deionized water to fit the COD detection range of 20 - 1,500 mg/L.

TDS: We estimated TDS by the following equation.

TDS (mg/L) = 0.67 mg-cm/L-mS × Electrical conductivity (µS/cm)   Equation (1)

We measured electrical conductivity by the electrometric method using a multi-parameter meter (HQ440D, HACH, Loveland, Colorado) (Rice et al., 2012).

pH: We measured pH by the electrometric method using a multi-parameter meter (HQ440D, HACH, Loveland, Colorado) (Rice et al., 2012).

BOD$_5$: We measured BOD$_5$ following the Standard Method 5210 Bby measuring the difference in dissolved oxygen concentration before and after a 5-day incubation at temperature of 25 ℃ (APHA, 2005). We measured dissolved oxygen by the electrometric method using a multi-parameter meter (HQ440D, HACH, Loveland, Colorado).

TSS: We measured TSS following the Standard Method 2540 D by filtering the samples (Whatman circular filters of 47 mm in diameter) and drying the filters by a benchtop muffle furnace (Thermolyne™) (APHA, 2005).

Ammonia: We measured ammonia by the salicylate method using ammonia salicylate and ammonia cyanurate reagents and a spectrophotometer (DR3900, Hach) (Adeniyi et al., 2023).

Metals: We measured zinc, arsenic, chromium by the Environmental Protection Agency (EPA) Method 3050B using a 4100 microwave plasma-atomic emission system (MP-AES) (U.S. EPA, 1996).

Organic contaminants: We measured α-terpineol, aniline, benzoic acid, naphthalene, p-cresol, phenol, pyridine by solid phase microextraction combined with gas chromatography–mass spectrometry (SPME-GC/MS) (Simões et al., 2007; Sagandykova et al., 2017). A Carboxen/Polydimethylsiloxane (CAR/PDMS) fiber was inserted in the headspace of a 60 mL vial. The glass vial was placed on a hotplate stirrer that was set at 400 revolutions per minutes and 75 °C for 20 minutes. Then, the fiber was inserted in the inlet of GC for the measurement.

Fluorotelomer alcohols (FTOHs): We measured FTOHs by headspace SPME-GC/MS. A CAR/PDMS fiber was inserted in the liquid of the 60 mL vial. The glass vial was placed on a hotplate stirrer that was set at 400 revolutions per minutes and 100 °C for 20 minutes (Tang et al., 2022). Then, the fiber was inserted in the inlet of GC for the measurement.

Other PFAS: We sent the samples to a commercial lab to measure 25 PFAS (Table 4). The method (Advanced Environmental Laboratories Standard Operation Procedure (AEL SOP-041) was isotope dilution anion exchange solid phase extraction combined with LC/MS/MS and was certified by the National Environmental Laboratory Accreditation Program.

Table 3. Methods for characterizing leachate residuals and condensates

Category	Parameters	Regulated by 40 CFR 445?	Method	Equipment	References
A) General physical parameters	TDS[1]	No	Electrometric method	Multi-parameter meter (HQ440D, Hach)	Rice et al., 2012
	TSS[2]	Yes	Standard Method 2540 D	Benchtop muffle furnace (Thermolyne™)	APHA, 2005
B) General chemical parameters	pH	Yes	Electrometric method	Multi-parameter meter (HQ440D, Hach)	Rice et al., 2012
	Ammonia	Yes	Salicylate method	Spectrophotometer (DR3900, Hach)	Adeniyi et al., 2023
	TOC[3]	No	Combustion catalytic oxidation	TOC analyzer (Shimadzu TOC-VCSH)	Opio et al., 2015
	COD[4]	No	Reactor digestion method (HACH method 8000)	Spectrophotometer (DR3900, Hach)	Elnakar and Buchanan, 2020
	BOD$_5$[5]	Yes	Standard Method 5210 B	Bottles with a ground-glass stopper	APHA, 2005
C) Metals	zinc, arsenic, chromium,	Yes	EPA[6] Method 3050B	4100 MP-AES[7] (Agilent Technologies)	U.S. EPA, 1996
D) Organic contaminants	α-terpineol, aniline, benzoic acid, naphthalene, p-cresol, phenol, pyridine,	Yes	Mass spectrometry method	GC/MS[8] (Agilent Technologies)	Simões et al., 2007
E) PFAS[9]	FTOHs[10]	No	Mass spectrometry method	GC/MS (Agilent Technologies)	Tang et al., 2022
	Other PFAS	No	AEL[12] SOP[13]-041	LC/MS/MS[11]	(Aellab Labs, 2023)

Notes:
[1] TDS = Total dissolved solids
[2] TSS = Total suspended solids
[3] TOC = Total organic carbon
[4] COD = Chemical oxygen demand
[5] BOD_5 = Five-day biochemical oxygen demand
[6] EPA = Environmental Protection Agency
[7] MP-AES = Microwave plasma-atomic emission system
[8] GC/MS = Gas chromatography mass spectrometry
[9] PFAS = Per- and polyfluoroalkyl substances
[10] FTOHs = Fluorotelomer alcohols
[11] LC/MS/MS = Liquid chromatography with mass spectrometry in tandem
[12] AEL = Advanced Environmental Laboratories, Inc.
[13] SOP = Standard operation procedure

Table 4. List of PFAS measured by liquid chromatography with tandem mass spectrometry (LC/MS/MS) (Zarebska et al., 2023)

Abbreviation	Compound	CAS[1]	Chemical formula	Molecular Mass, g/mol	Water solubility, mg/L
PFDoA	Perfluorododecanoic acid	307-55-1	$C_{11}F_{23}COOH$	614	0.71
PFUnA	Perfluoroundecanoic acid	2058-94-8	$C_{10}F_{21}COOH$	564	4.2
PFDA	Perfluorodecanoic acid	335-76-2	$C_9F_{19}COOH$	514	25
PFNA	Perfluorononanoic acid	375-95-1	$C_8F_{17}COOH$	464	131
PFOA	Perfluorooctanoic acid	335-67-1	$C_7F_{15}COOH$	414	771
PFHpA	Perfluoroheptanoic acid	375-85-9	$C_6F_{13}COOH$	364	4,180
PFHxA	Perfluorohexanoic acid	307-24-4	$C_5F_{11}COOH$	314	22,000
PFPeA	Perfluoropentanoic acid	2706-90-3	C_4F_9COOH	264	110,000
PFBA	Perfluorobutanoic acid	375-22-4	C_3F_7COOH	214	560,000
PFOS	Perfluorooctane sulfonic acid	1763-23-1	$C_8F_{17}SO_3H$	500	60
PFHpS	Perfluoroheptane sulfonic acid	375-92-8	$C_7F_{15}SO_3H$	450	-
PFHxS	Perfluorohexane sulfonic acid	355-46-4	$C_6F_{13}SO_3H$	400	2,300
PFPeS	Perfluoropentane sulfonic acid	2706-91-4	$C_5F_{11}SO_3H$	350	-
PFBS	Perfluorobutane sulfonic acid	375-73-5	$C_4F_9SO_3H$	300	30,000
4:2 FTS	4:2 fluorotelomer sulfonic acid	757124-72-4	$C_6H_5F_9O_3S$	328	28,000
6:2 FTS	6:2 fluorotelomer sulfonic acid	27619-97-2	$C_8H_5F_{13}O_3S$	428	1,320
8:2 FTS	8:2 fluorotelomer sulfonic acid	39108-34-4	$C_{10}H_5F_{17}O_3S$	528	58
9Cl-PF3ONS	9-Chlorohexadecafluoro-3-oxanonane-1-sulfonic acid	7569426-58-1	$C_8HClF_{16}O_4S$	531	-
11Cl-PF3OUdS	11-Chloroeicosafluoro-3-oxaundecane-1-sulfonic acid	763051-92-9	$C_{10}HClF_{20}O_4S$	632	-
ADONA	4,8-dioxa-3Hperfluorononanoic acid	919005-14-4	$C_7H_2F_{12}O_4$	378	3,150
HFPO-DA	Hexafluoropropylene oxide dimer acid	13252-13-6	$C_5F_{11}OCOOH$	330	7,060
NFDHA	Nonafluoro-3,6-dioxaheptanoic acid	151772-58-6	$C_5HF_9O_4$	296	-
PFEESA	Perfluoro (2-ethoxyethane) sulfonic acid	113507-82-7	$C_4HF_9O_4S$	316	-
PFMBA	Perfluoro-3-methoxypropanoic acid	377-73-1	$C_4HF_7O_3$	230	-
PFMPA	Perfluoro-4-methoxybutanoic acid	863090-89-5	$C_5HF_9O_3$	280	-

Note:
[1] CAS = Chemical abstracts service

3. RESULTS AND DISCUSSION

3.1. Effects of leachate evaporation on the fate of PFAS and contaminants regulated by 40 CFR 445.11 (Task 1)

After evaporating three leachates sampled from three landfills, respectively, in Florida, we collected leachate residuals and condensates. We measured various compounds following the methods mentioned in Table 3. As mentioned before, we classified the compounds in 5 groups, including general physical parameters, general chemical parameters, metals, organic contaminants, and PFAS. We discuss the results for each group below.

Category 1 -- general physical parameters: As shown in Figure 4, TDS increased in all leachate residuals by increase of evaporation percentage. However, the TDS decreased in condensates with the increase of evaporation. The highest TDS concentration in all condensates was observed at 12.5% evaporation. Then TDS decreased as the evaporation percentage increased. It happened because volatile portions of TDS have been transferred from leachate residual to condensate at the beginning of the evaporation. As evaporation continued, more dilution happened, and the concentration of TDS in condensates decreased. The pattern of TSS in the leachate residual was like TDS: Higher evaporation percentages led to increased TSS in the leachate residuals. However, the TSS was below the detection limit of 15 mg/L in all condensates, suggesting that TSS cannot be transferred from leachate to condensate. Figure A1 shows the mass balance for TDS and TSS. As shown in Figure A1, more than 50% of TDS and TSS remained in residual. Therefore, TDS and TSS accumulated in residual during leachate evaporation.
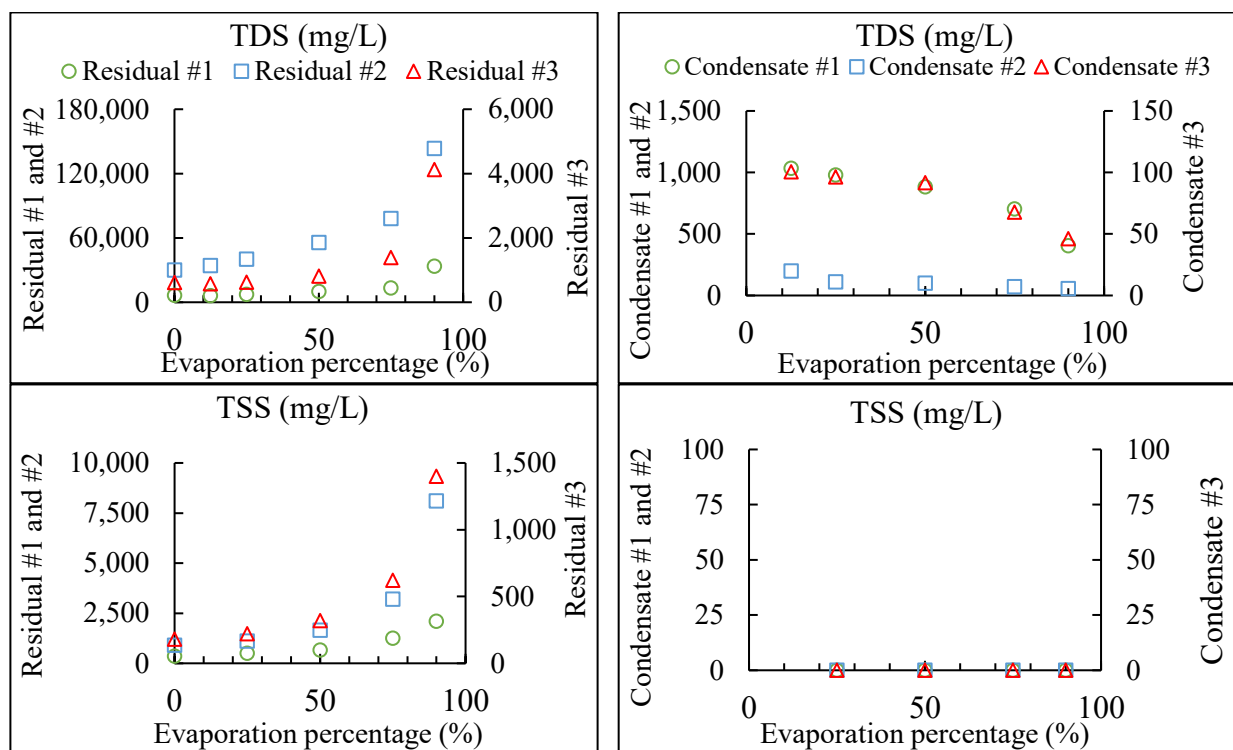

Figure 4. General physical parameters in the leachate residual (left) and condensate (right)

13

Category 2 -- general chemical parameters: As shown in Figure 5, we observed different patterns for pH in different leachates. pH was 8.35 in residual #1 at 0% evaporation, and slowly increased by increase of evaporation percentage. At 90% evaporation, pH in residual #1 reached 9.36. The pattern in leachate residual #3 was similar: pH increased from 8.14 at 0% evaporation to 9.03 at 90% evaporation. However, the pattern in leachate residual #2 was different, and pH decreased from 7.49 at 0% evaporation to 4.26 at 90% evaporation. Similarly, the pattern of pH in the condensate also depended on the leachate.

Ammonia is a semi-volatile compound, and its concentration in all three leachate residuals decreased continuously and reached 2 mg/L, 32.8 mg/L, and below the detection limit of 1 mg/L at 90 % evaporation in residual #1, residual #2, and residual #3, respectively. Evaporation of leachate is a method for the removal of ammonia from landfill leachate because ammonia can be removed by volatilization and decomposition (García., et al., 2013; Zhang et al., 2022). The highest concentration of ammonia in the condensate was observed at 12.5 % evaporation. Then, it decreased because of dilution and further volatilization in the condenser. Figure A2 shows the mass balance for ammonia in the three leachates. The mass balance shows that ammonia initially went to the condensate and then to the gas phase.

As the evaporation progressed, the concentration of TOC, COD, and BOD_5 increased in the leachate residual because of the decrease of residual volume. However, some TOC, COD, and BOD_5 were volatile and escaped to the condenser. At the beginning of evaporation, a significant amount of volatile TOC, COD, and BOD_5 in leachate residual was transferred to the condensate, leading to the highest concentration of TOC, COD, and BOD_5 observed at 12.5% evaporation. When evaporation continued, the concentration of TOC, COD, and BOD_5 in the condenser decreased because of dilution. Figure A2 shows the mass balance for TOC, COD, and BOD_5 in the three leachates. The mass balance shows that more than 50% of TOC, COD, and BOD_5 remained in the residuals expect for BOD_5 in one leachate. Therefore, TOC, COD, and BOD_5 accumulated in the leachate residual.
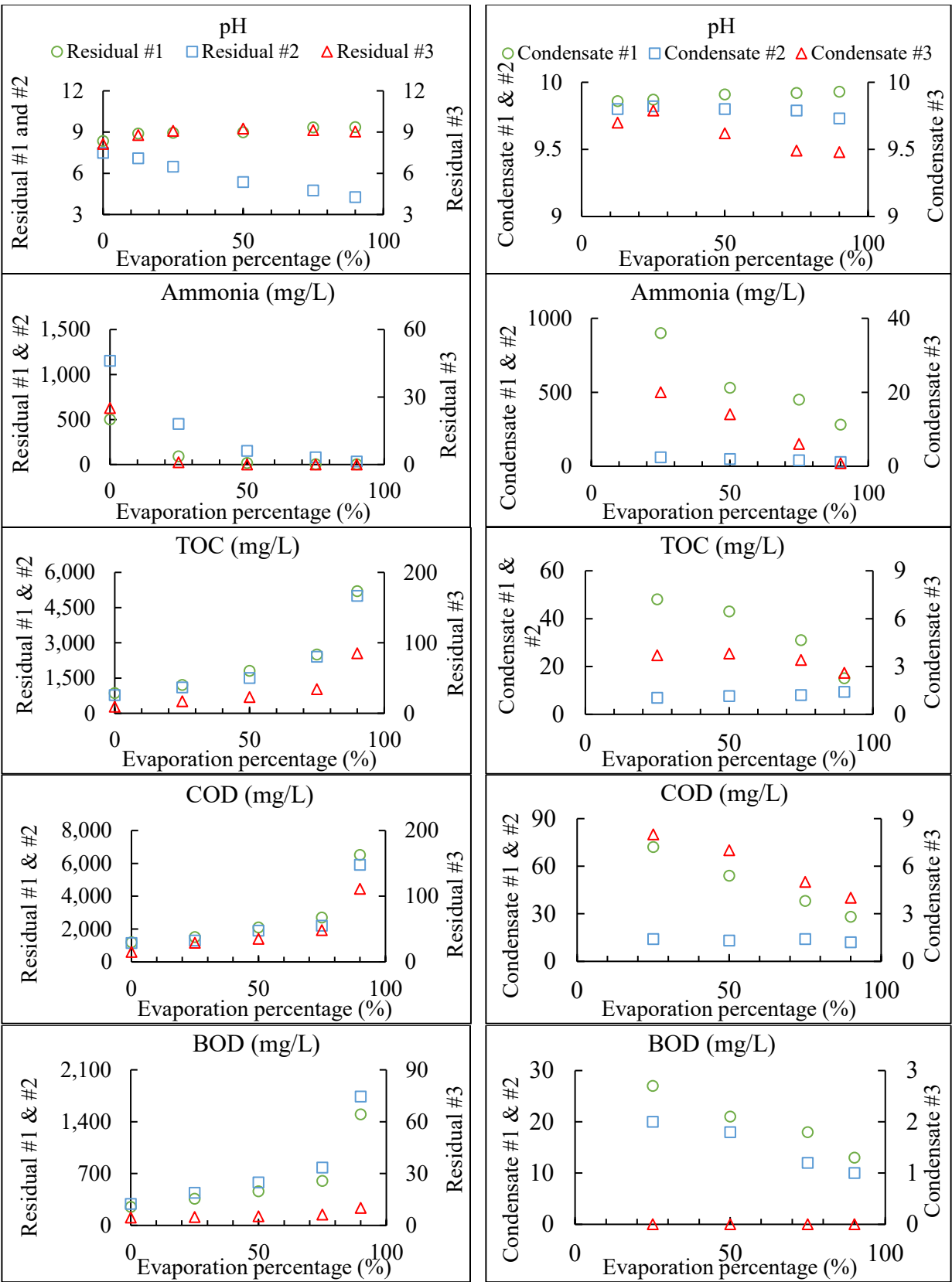
Figure 5. General chemical parameters in the leachate residual (left) and condensate (right)

Category 3 -- metals: As shown in Figure 6, the concentrations of zinc and chromium increased in the leachate residuals. We did not detect any zinc and chromium in the condensates, suggesting these metals were not volatile and they were not transferred to the condensate. The detection limit for zinc, chromium, and arsenic was 10 µg/L, 10 µg/L, and 100 µg/L, respectively. Figure A3 shows the mass balance for metals. More than 50% of zinc and chromium were shown as "other". This portion of metals likely precipitated due to the concentration in the residuals and firmly attached to the bottom of the evaporator; therefore, they were not measured as leachate residuals, but they were likely part of the residuals.
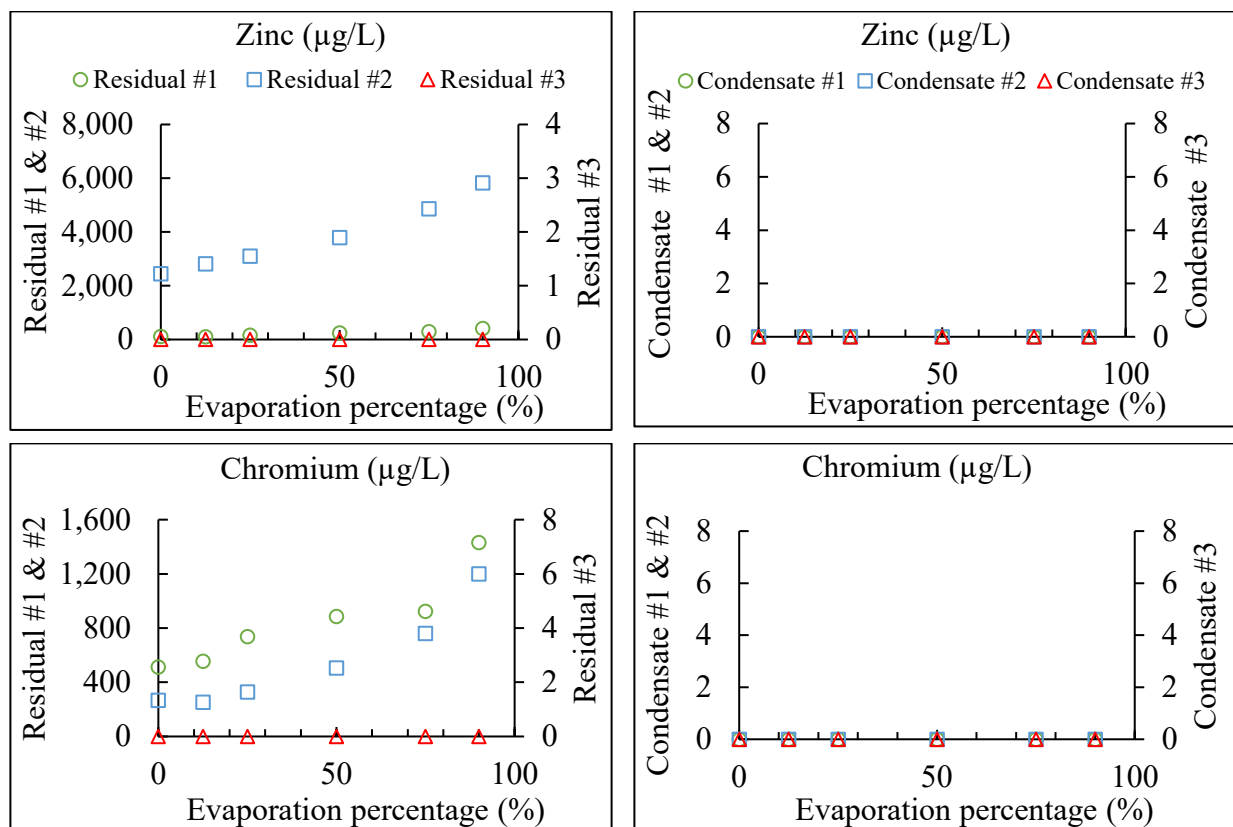
Figure 6. Metals in the leachate residual (left) and condensate (right). Arsenic was below the detection limit of 100 µg/L.

Category 4 -- organic compounds: We measured α-terpineol, benzoic acid, naphthalene, p-cresol, pyridine, aniline, and phenol in the residual and condensate of the three leachates. The results are shown in Figure 7. The concentrations of α-terpineol and benzoic acid in all samples were below the detection limit of 0.200 µg/L and 4,000 µg/L, respectively. The pattern of change for naphthalene, p-cresol, and pyridine were the same: Their concentrations were decreasing in both leachate residual and condensate for all three leachates. They are common in that they have high volatility associated with high vapor pressure: 102 mmHg for naphthalene and p-cresol, and 24.8 mmHg for pyridine (Stull., 1947). The patterns of change for aniline and phenol depended on the leachate: This might be due to the fact that they could be reaction products (Figoli et al., 1982; Taniguchi et al., 2015), which increased the complexity. More details are discussed below.

16

Naphthalene was detected in leachate #1 and leachate #2. The concentration of naphthalene in residual leachate #1 and residual leachate #2 at 0% evaporation was 2.20 µg/L and 1.60 µg/L, respectively. The concentration of naphthalene in residual #1 and residual #2 decreased to below its detection limit after 12.5 % evaporation. It is because of the high volatility of naphthalene that is associated with its high vapor pressure (102 mmHg) (Stull., 1947). The concentration of naphthalene in condensate #1 and condensate #2 at 12.5% evaporation was 2.40 µg/L and 1.78 µg/L, respectively. Because of volatility of naphthalene and dilution, the concentration of naphthalene in condensate reached below the detection limit after 25% evaporation. Mass balance (Figure A4-A) shows that all naphthalene went to the gas phase after 90% evaporation.

The concentration of p-cresol in leachate residual #1, residual #2, and residual #3 at 0% evaporation was 5.97 µg/L, 5.25 µg/L, and 0.215 µg/L, respectively. As the evaporation progressed, the concentration of p-cresol decreased in the three residuals and reached to below the detection limit of 0.200 µg/L at 90% evaporation. The decrease of p-cresol in leachate residuals is associated with its high vapor pressure (102 mmHg) (Stull., 1947). On the other hand, we observed the highest concentration of p-cresol in condensates at 12.5 % evaporation. The concentration of p-cresol in condensate #1, condensate #2, and condensate #3 at 12.5% evaporation was 15.3, 14.2, and 0.570 µg/L. The p-cresol concentration in the condensates decreased because of dilution in the condensate collector. The concentration of p-cresol at 90 % evaporation was 5.52 µg/L, 5.48 µg/L, and 0.227 µg/L, respectively. Mass balance (Figure A4-B) shows that more than 80% of the initial p-cresol mass went to the condensate after 90% evaporation.

At 0% evaporation, the pyridine concentration in leachate residual #1, residual #2, and residual #3 was at 10.8 µg/L, 47.0 µg/L, and 3.35 µg/L, respectively. As the evaporation process advanced, the pyridine concentration steadily declined in these three residuals, ultimately dropping below the detection limit of 0.500 µg/L when the evaporation reached 50%. The decrease in pyridine levels within the leachate residuals could be attributed to the high volatility of pyridine, resulting from its high vapor pressure (24.8 mmHg) (Stull., 1947). We observed the highest concentration of p-cresol in condensates at 12.5 % evaporation. At this time, the pyridine concentration in condensates #1, #2, and #3 was 82.6 µg/L, 168 µg/L, and 13.0 µg/L, respectively. Pyridine concentration continuously decreased in the condensates because of dilution occurring within the condensate collector. At 90% evaporation, the pyridine concentrations in condensates #1, #2, and #3 reached 9.62 µg/L, 27.4 µg/L, and 1.80 µg/L, respectively. Mass balance (Figure A4-C) shows that around 50% of the initial pyridine mass went to the condensate and the rest to the gas phase after 90% evaporation.

In leachate residual #1, the concentration of aniline increased from below the detection limit of 0.250 µg/L to 0.310 µg/L. There may be two reasons. First, aniline could be generated because of some reactions. Second, the rate of volatilization of aniline in leachate residual #1, could be lower than the rate of the leachate residual volume decrease. The concentration of aniline in leachate residual #2 continuously decreased, probably due to aniline volatility. Because of its high vapor pressure (82 mmHg) (Stull., 1947), the escape of aniline from leachate residual was expected. The aniline concentration in condensate #1 increased from 12.5% to 50% evaporation

and then decreased. However, the concentration of aniline in condensate #2 continuously decreased. Aniline in residual leachate #3 and condensate #3 was below the detection limit of 0.250 µg/L all the time. Mass balance (Figure A4-D) shows that aniline in the condensate after 90% evaporation could be higher than its initial mass in the leachate, suggesting that it might be produced due to reactions.

The concentration of phenol in leachate residual #1 increased from 0.173 µg/L at 0% evaporation to 0.899 µg/L at 90% evaporation. It could be because of the reactions in the leachate, leading to the production of phenol. In leachate residual #2, the concentration of phenol decreased from 0.590 µg/L to 0.182 µg/L. In both condensate #1 and condensate #2, the highest concentration of phenol was observed at 50% evaporation. At this time, the concentration of phenol in condensate #1 and condensate #2 was 0.494 µg/L and 0.650 µg/L, respectively. The phenol concentration was below the detection limit of 0.150 µg/L in the leachate residual #3 and condensate #3 all the time. Mass balance (Figure A4-E) shows that phenol in the condensate after 90% evaporation could be higher than its initial mass in the raw leachate, suggesting that it might be produced due to reactions.
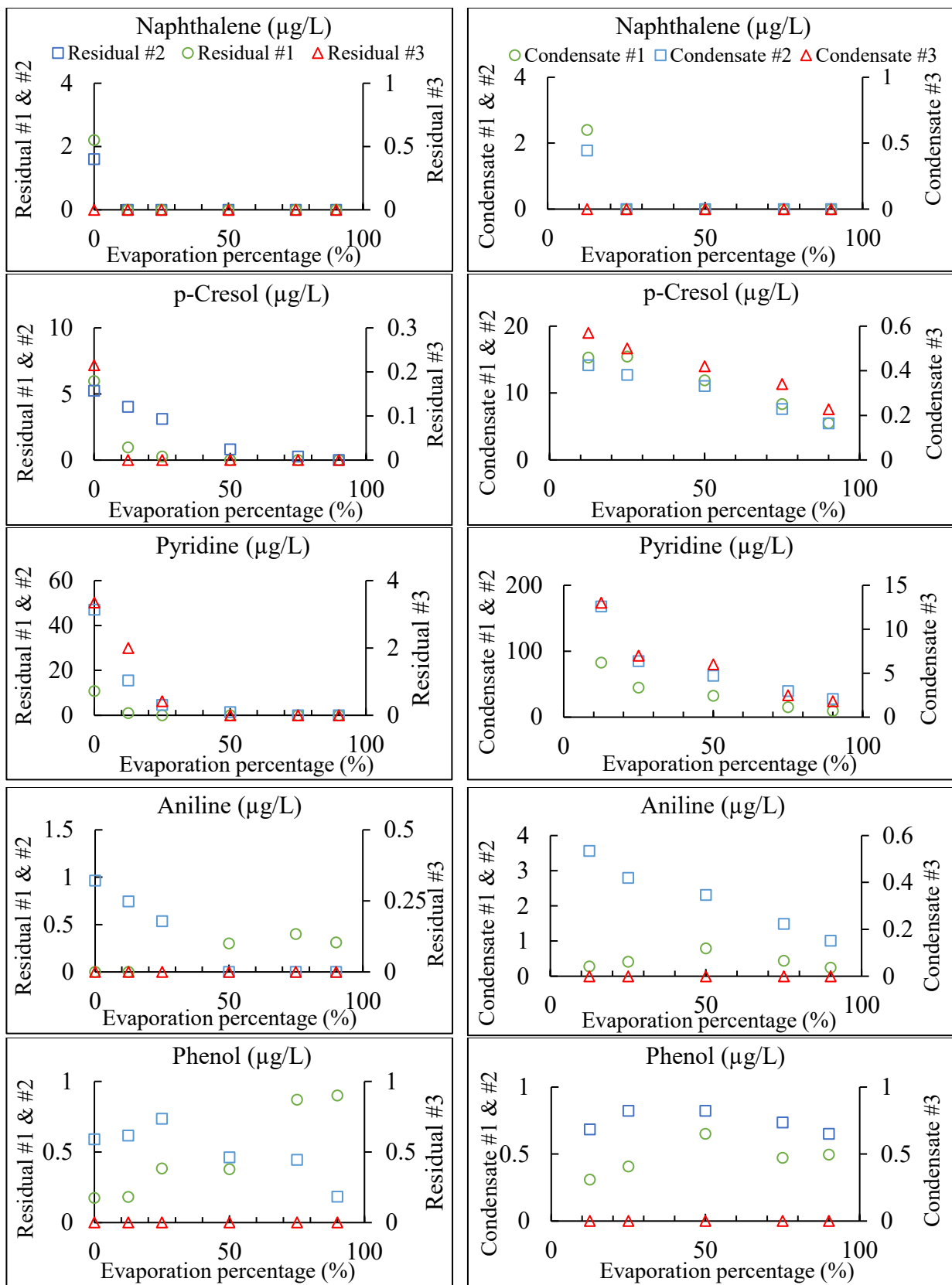
Figure 7. Organic comounds in the leachate residual (left) and condensate (right). Benzoic acid and α-terpineol were below detection limit of 0.200 µg/L and 4,000 µg/L, respectively.

Category 5 -- PFAS: We divided PFAS into two sub-groups, including FTOHs (measured by GC/MS) and other PFAS (measured by LC/MS/MS).

FTOHs: At 0% evaporation, we detected 6:2 FTOH 0.021 µg/L in leachate residual #2 as shown in Figure 8. The concentration of 6:2 FTOH reached below the detection limit of 0.006 µg/L after 12.5% evaporation. In the leachate residuals, the concentration of 4:2 FTOH, 8:2 FTOH, and 10:2 FTOH were below the detection limits of 0.020 µg/L, 0.006 µg/L, and 0.020 µg/L, respectively. Moreover, we did not detect any FTOHs in the condensates. Mass balance (Figure A5) shows that 6:2 FTOH mass went to the gas phase after 90% evaporation.
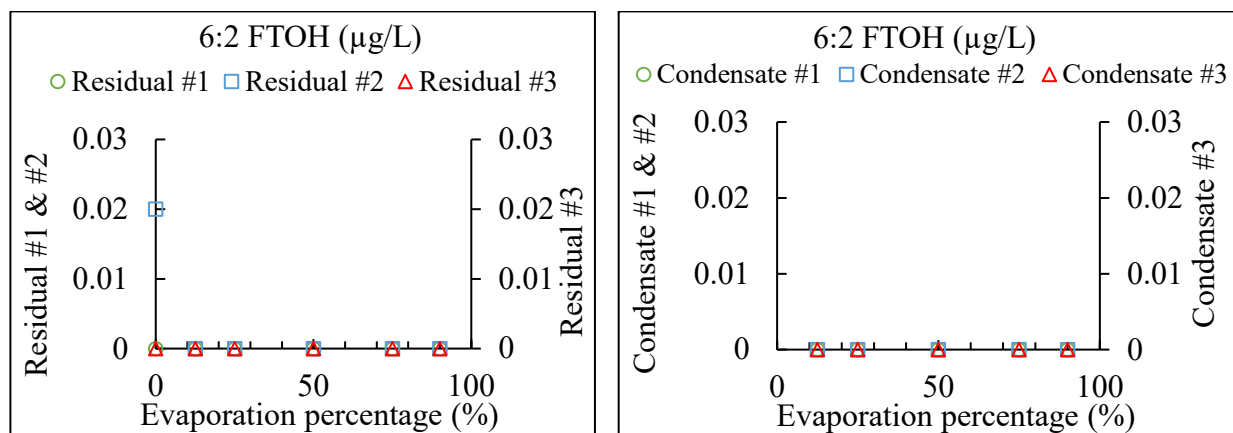
Figure 8. FTOHs in the leachate residual (left) and condensate (right). 4:2 FTOH, 8:2 FTOH, and 10:2 FTOH were below the detection limit of 0.020 µg/L, 0.006 µg/L, and 0.020 µg/L, respectively.

Other PFAS: We observed similar patterns for leachate #1 and leachate #2. Nine of the 25 PFAS measured by LC/MS/MS were above their detection limits in the leachate residual #1 (Table 5). Eight of the 25 PFAS were above their detection limits in leachate residual #2 (Table 6). The removal percentages (based on concentration) of these PFAS were between -710% and -1,070% in the leachate residual #1, and between -661% and -1,080% in leachate residual #2. The removal percentages (based on mass) of these PFAS were between -16.7% and 19% in leachate residual #1, and -18.4% and 23.9% in leachate residual #2. PFAS accumulated in the leachate residuals as the evaporation progressed. We did not detect any PFAS in condensates #1 and #2, suggesting that these PFAS could not transfer to the condensates.

At 0% evaporation, we did not detect any PFAS in leachate residual #3 as shown in Table 7. However, we detected ten PFAS in the leachate residual after 90% evaporation. Their concentrations ranged between 0.120-0.950 µg/L. Because the volume of residual decreased by evaporation, the concentration of PFAS could increase from below the detection limits to detectable values.

Table 5. Concentrations and removal percentages of PFAS in leachate #1

PFAS	Concentration (µg/L)			Removal percentage (%)	
	Residual at 0%	Residual at 90%	Condensate at 90%	Based on concentration[1]	Based on mass[2]
4:2 FTS[5]	BDL[3]	**2.00**	BDL	N.C.[4]	-
6:2 FTS[6]	**4.30**	**38.0**	BDL	-784	11.6
8:2 FTS[7]	BDL	BDL	BDL	-	-
9Cl-PF3ONS[8]	BDL	BDL	BDL	-	-
11Cl-PF3OUdS[9]	BDL	BDL	BDL	-	-
ADONA[10]	BDL	BDL	BDL	-	-
HFPO-DA[11]	BDL	BDL	BDL	-	-
NFDHA[12]	BDL	BDL	BDL	-	-
PFEESA[13]	BDL	BDL	BDL	-	-
PFMBA[14]	BDL	BDL	BDL	-	-
PFMPA[15]	BDL	BDL	BDL	-	-
PFOS[16]	BDL	**1.20**	BDL	N.C.	-
PFHpS[17]	BDL	BDL	BDL	-	-
PFHxS[18]	**0.740**	**7.90**	BDL	-968	-6.76
PFPeS[19]	BDL	**1.30**	BDL	N.C.	-
PFBS[20]	**1.50**	**16.0**	BDL	-967	-6.67
PFDoA[21]	BDL	BDL	BDL	-	-
PFUnA[22]	BDL	BDL	BDL	-	-
PFDA[23]	BDL	BDL	BDL	-	-
PFNA[24]	**1.80**	**15.0**	BDL	-733	16.7
PFOA[25]	**1.10**	**9.30**	BDL	-745	15.4
PFHpA[26]	**0.550**	**5.60**	BDL	-918	-1.82
PFHxA[27]	**3.20**	**34.0**	BDL	-963	-6.25
PFPeA[28]	**1.20**	**14.0**	BDL	-1,070	-16.7
PFBA[29]	**2.10**	**17.0**	BDL	-710	19.0

[1] Removal percentage in leachate residual based on concentration was calculated by (concentration in residual at 0% evaporation - concentration in residual at 90% evaporation)/ concentration in residual at 0% evaporation.

[2] Removal percentage in leachate residual based on mass was calculated by (concentration in residual at 0% evaporation × volume of residual at 0% evaporation - concentration in residual at 90% × concentration in residual at 90%)/ (concentration in residual at 0% evaporation × volume of residual at 0% evaporation).

[3] BDL = Below detection limit. The detection limit for residual at 0%, residual at 90%, and condensate at 90% was 0.220 µg/L, 1.00 µg/L, and 0.100 µg/L, respectively.

[4] N.C. = Not calculated. The denominator is zero.

[5] 4:2 FTS= 4:2 Fluorotelomer sulfonate; [6] 6:2 FTS= 6:2 Fluorotelomer sulfonate; [7] 8:2 FTS= 8:2 Fluorotelomer sulfonate; [8] 9Cl-PF3ONS= 9-Chlorohexadecafluoro-3-oxanonane-1-sulfonic acid; [9] 11Cl-PF3OUdS= 11-Chloroeicosafluoro-3-oxaundecane-1-sulfonic acid; [10] ADONA= 4,8-dioxa-3Hperfluorononanoic Acid; [11] HFPO-DA= Hexafluoropropylene oxide dimer acid; [12] NFDHA= Nonafluoro-3,6-dioxaheptanoic acid; [13] PFEESA= Perfluoro (2-ethoxyethane) sulfonic acid; [14] PFMBA= Perfluoro-3-methoxypropanoic acid; [15] PFMPA= Perfluoro-4-methoxybutanoic acid; [16] PFOS= Perfluorooctane sulfonic acid; [17] PFHpS= Perfluoroheptane sulfonic acid; [18] PFHxS= Perfluorohexane sulfonic acid; [19] PFPeS= Perfluoropentane sulfonic acid; [20] PFBS= Perfluorobutane sulfonic acid; [21] PFDoA= Perfluorododecanoic acid ; [22] PFUnA= Perfluoroundecanoic acid ; [23] PFDA= Perfluorodecanoic acid; [24] PFNA= Perfluorononanoic acid; [25] PFOA= Perfluorooctanoic acid; [26] PFHpA= Perfluoroheptanoic acid; [27] PFHxA= Perfluorohexanoic acid; [28] PFPeA= Perfluoropentanoic acid; [29] PFBA= Perfluorobutanoic acid

Table 6. Concentrations and removal percentages of PFAS in leachate #2

PFAS	Concentration (µg/L)			Removal percentage (%)	
	Residual at 0%	Residual at 90%	Condensate at 90%	Based on concentration[1]	Based on mass[2]
4:2 FTS[4]	BDL[3]	BDL	BDL	-	-
6:2 FTS[5]	**0.290**	**2.25**	BDL	-676	22.4
8:2 FTS[6]	BDL	BDL	BDL	-	-
9Cl-PF3ONS[7]	BDL	BDL	BDL	-	-
11Cl-PF3OUdS[8]	BDL	BDL	BDL	-	-
ADONA[9]	BDL	BDL	BDL	-	-
HFPO-DA[10]	BDL	BDL	BDL	-	-
NFDHA[11]	BDL	BDL	BDL	-	-
PFEESA[12]	BDL	BDL	BDL	-	-
PFMBA[13]	BDL	BDL	BDL	-	-
PFMPA[14]	BDL	BDL	BDL	-	-
PFOS[15]	BDL	BDL	BDL	-	-
PFHpS[16]	**0.750**	**7.05**	BDL	-840	6.00
PFHxS[17]	BDL	BDL	BDL	-	-
PFPeS[18]	BDL	BDL	BDL		-
PFBS[19]	**7.30**	**76.5**	BDL	-948	-4.79
PFDoA[20]	BDL	BDL	BDL	-	-
PFUnA[21]	BDL	BDL	BDL	-	-
PFDA[22]	BDL	BDL	BDL	-	-
PFNA[23]	BDL	BDL	BDL	-	-
PFOA[24]	**0.710**	**5.40**	BDL	-661	23.9
PFHpA[25]	**0.490**	**3.75**	BDL	-665	23.5
PFHxA[26]	**2.50**	**22.5**	BDL	-800	10
PFPeA[27]	**1.20**	**12.0**	BDL	-900	0
PFBA[28]	**1.90**	**22.5**	BDL	-1080	-18.4

[1] Removal percentage in leachate residual was calculated by (concentration in residual at 0% evaporation - concentration in residual at 90% evaporation)/ concentration in residual at 0% evaporation.

[2] Removal percentage in leachate residual based on mass was calculated by (concentration in residual at 0% evaporation × volume of residual at 0% evaporation - concentration in residual at 90% × concentration in residual at 90%)/ (concentration in residual at 0% evaporation × volume of residual at 0% evaporation).

[3] BDL = Below detection limit. The detection limit for residual at 0%, residual at 90%, and condensate at 90% was 0.100 µg/L, 1.5 µg/L, and 0.100 µg/L, respectively.

[4] 4:2 FTS= 4:2 Fluorotelomer sulfonate; [5] 6:2 FTS= 6:2 Fluorotelomer sulfonate; [6] 8:2 FTS= 8:2 Fluorotelomer sulfonate; [7] 9Cl-PF3ONS= 9-Chlorohexadecafluoro-3-oxanonane-1-sulfonic acid; [8]11Cl-PF3OUdS= 11-Chloroeicosafluoro-3-oxaundecane-1-sulfonic acid; [9] ADONA= 4,8-dioxa-3Hperfluorononanoic Acid; [10] HFPO-DA= Hexafluoropropylene oxide dimer acid; [11]NFDHA= Nonafluoro-3,6-dioxaheptanoic acid; [12]PFEESA= Perfluoro (2-ethoxyethane) sulfonic acid; [13]PFMBA= Perfluoro-3-methoxypropanoic acid; [14] PFMPA= Perfluoro-4-methoxybutanoic acid; [15] PFOS= Perfluorooctane sulfonic acid; [16] PFHpS= Perfluoroheptane sulfonic acid; [17] PFHxS= Perfluorohexane sulfonic acid; [18] PFPeS= Perfluoropentane sulfonic acid; [19] PFBS= Perfluorobutane sulfonic acid; [20] PFDoA= Perfluorododecanoic acid ; [21]PFUnA= Perfluoroundecanoic acid ; [22]PFDA= Perfluorodecanoic acid; [23] PFNA= Perfluorononanoic acid; [24] PFOA= Perfluorooctanoic acid; [25] PFHpA= Perfluoroheptanoic acid; [26] PFHxA= Perfluorohexanoic acid; [27] PFPeA= Perfluoropentanoic acid; [28] PFBA= Perfluorobutanoic acid.

Table 7. Concentrations and removal percentages of PFAS in leachate #3

PFAS	Concentration (µg/L)			Removal percentage (%)	
	Residual at 0%	Residual at 90%	Condensate at 90%	Based on concentration[1]	Based on mass[2]
4:2 FTS[5]	BDL[3]	BDL	BDL	-	-
6:2 FTS[6]	BDL	BDL	BDL	-	-
8:2 FTS[7]	BDL	**370**	BDL	N.C.[4]	N.C.
9Cl-PF3ONS[8]	BDL	BDL	BDL	-	-
11Cl-PF3OUdS[9]	BDL	BDL	BDL	-	-
ADONA[10]	BDL	BDL	BDL	-	-
HFPO-DA[11]	BDL	**130**	BDL	N.C.	N.C.
NFDHA[12]	BDL	BDL	BDL	-	-
PFEESA[13]	BDL	BDL	BDL	-	-
PFMBA[14]	BDL	BDL	BDL	-	-
PFMPA[15]	BDL	BDL	BDL	-	-
PFOS[16]	BDL	**950**	BDL	N.C.	N.C.
PFHpS[17]	BDL	BDL	BDL	-	-
PFHxS[18]	BDL	**110**	BDL	N.C.	N.C.
PFPeS[19]	BDL	BDL	BDL	-	-
PFBS[20]	BDL	**110**	BDL	N.C.	N.C.
PFDoA[21]	BDL	BDL	BDL	-	-
PFUnA[22]	BDL	BDL	BDL	-	-
PFDA[23]	BDL	**510**	BDL	N.C.	N.C.
PFNA[24]	BDL	**120**	BDL	N.C.	N.C.
PFOA[25]	BDL	**440**	BDL	N.C.	N.C.
PFHpA[26]	BDL	**470**	BDL	N.C.	N.C.
PFHxA[27]	BDL	**120**	BDL	N.C.	N.C.
PFPeA[28]	BDL	BDL	BDL	-	-
PFBA[29]	BDL	BDL	BDL	-	-

[1] Removal percentage in leachate residual was calculated by (concentration in residual at 0% evaporation - concentration in residual at 90% evaporation)/ concentration in residual at 0% evaporation.

[2] Removal percentage in leachate residual based on mass was calculated by (concentration in residual at 0% evaporation × volume in residual at 0% evaporation - concentration in residual at 90% × concentration in residual at 90% evaporation)/ (concentration in residual at 0% evaporation × volume of residual at 0% evaporation).

[3] BDL = Below detection limit. The detection limit for residual at 0%, residual at 90%, and condensate at 90% was 0.100 µg/L.

[4] N.C. = Not calculated. The denominator is zero.

[5] 4:2 FTS= 4:2 Fluorotelomer sulfonate; [6] 6:2 FTS= 6:2 Fluorotelomer sulfonate; [7] 8:2 FTS= 8:2 Fluorotelomer sulfonate; [8] 9Cl-PF3ONS= 9-Chlorohexadecafluoro-3-oxanonane-1-sulfonic acid; [9] 11Cl-PF3OUdS= 11-Chloroeicosafluoro-3-oxaundecane-1-sulfonic acid; [10] ADONA= 4,8-dioxa-3Hperfluorononanoic Acid; [11] HFPO-DA= Hexafluoropropylene oxide dimer acid; [12] NFDHA= Nonafluoro-3,6-dioxaheptanoic acid; [13] PFEESA= Perfluoro (2-ethoxyethane) sulfonic acid; [14] PFMBA= Perfluoro-3-methoxypropanoic acid; [15] PFMPA= Perfluoro-4-methoxybutanoic acid; [16] PFOS= Perfluorooctane sulfonic acid; [17] PFHpS= Perfluoroheptane sulfonic acid; [18] PFHxS= Perfluorohexane sulfonic acid; [19] PFPeS= Perfluoropentane sulfonic acid; [20] PFBS= Perfluorobutane sulfonic acid; [21] PFDoA= Perfluorododecanoic acid ; [22] PFUnA= Perfluoroundecanoic acid ; [23] PFDA= Perfluorodecanoic acid; [24] PFNA= Perfluorononanoic acid; [25] PFOA= Perfluorooctanoic acid; [26] PFHpA= Perfluoroheptanoic acid; [27] PFHxA= Perfluorohexanoic acid; [28] PFPeA= Perfluoropentanoic acid; [29] PFBA= Perfluorobutanoic acid

3.2. Distribution ratios of PFAS (Task 2)

The behavior of PFAS in terms of volatilization and partitioning during thermal treatment varies based on factors such as the alkyl chain length and the functional group (Crownover et al., 2019). We here evaluated their partition during the evaporation process.

Distribution of FTOHs: After 12.5% of evaporation, more than 99.9% the FTOH mass went to the gas phase (Figure 9C). At 50% of evaporation, the concentrations of all FTOHs in the synthetic leachate residual reached below their detection limits (Figure 9A). FTOHs have high vapor pressures and henry constants (Abusallout et al., 2022); therefore, they can easily escape from the leachate residual at high temperatures. The concentrations of FTOHs in the condensate was high at the start of evaporation because of input from the leachate residual and then decreased due to the vacuum-caused evaporation and dilution in the condensate collector (Figure 9B).
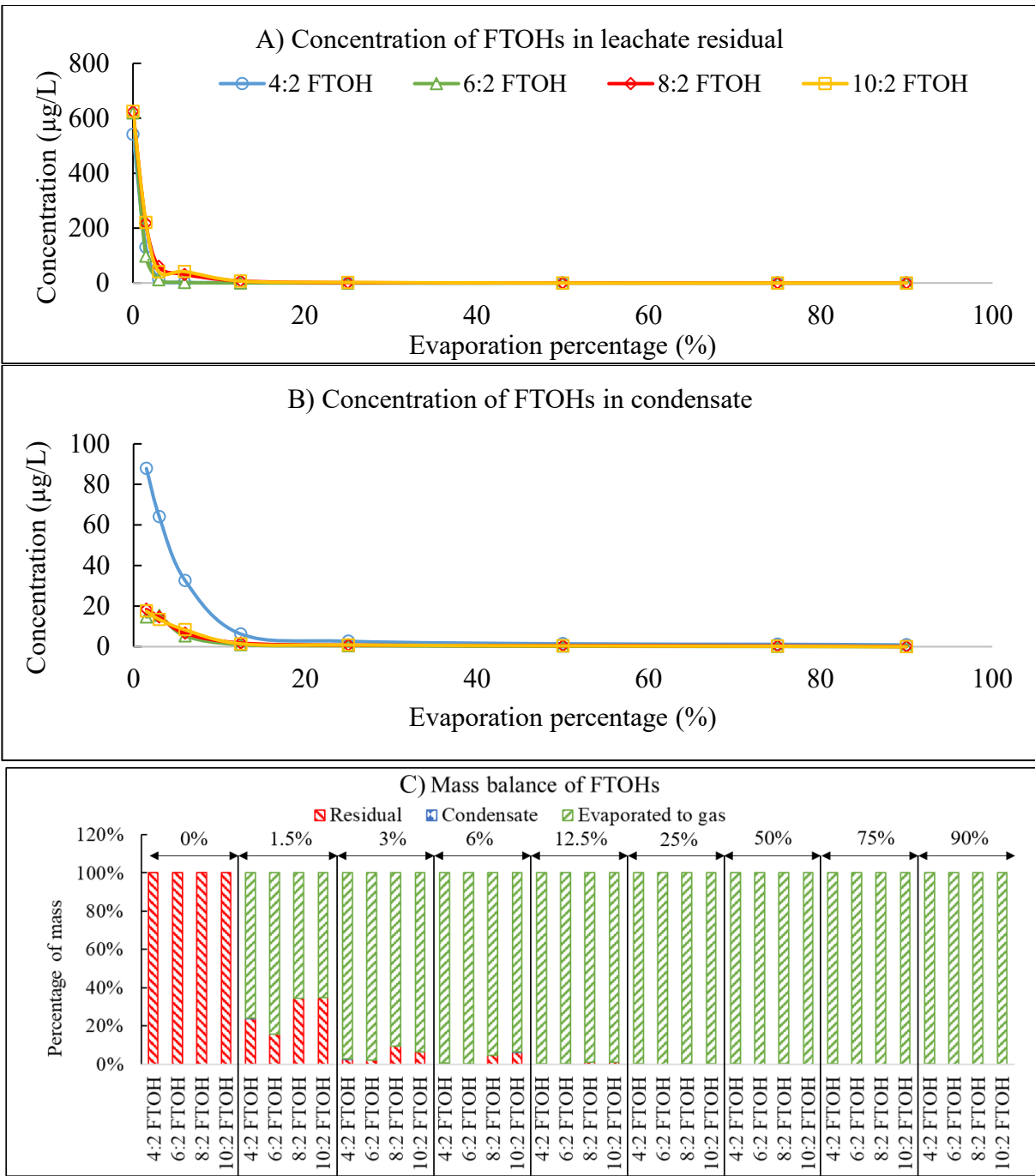
Figure 9. The concentrations of FTOHs in residual (A) and condensate (B) and the mass balance of FTOHs (C) during evaporation.

Distribution of PFCAs: Table 8 shows the concentrations of PFCAs in the leachate residual at 0%, residual at 90%, and condensate at 90% for the synthetic leachate. The concentrations of PFCAs increased by 7.8 to 12 times in the leachate residual due to the volume reduction by 90%. A very small portion of PFCAs (0.7 - 37 µg/L) were transferred to the condensate. Compared to FTOHs, PFCAs have lower vapor pressures and henry constants. Therefore, they are less likely to be transferred to the condensate.

To calculate the ratio of the mass of PFCA in leachate residual and condensate to initial mass of PFAS, we used the following formula:

$$P_R = \frac{C_{R,90\%}V_{R,90\%}}{C_I V_I} \times 100 \qquad \text{Equation (2)}$$

$$P_C = \frac{C_{C,90\%}V_{C,90\%}}{C_I V_I} \times 100 \qquad \text{Equation (3)}$$

P_R is the percentage of PFCA mass in leachate residual. $C_{R,\,90\%}$ is the concentration of PFCA in leachate residual at 90% evaporation. $V_{R,\,90\%}$ is the volume of leachate residual at 90% evaporation. C_I is the concentration of PFCA in leachate residual at 0% evaporation. V_I is the volume of leachate residual at 0% evaporation. P_C is the percentage of PFCA mass in condensate. $C_{C,\,90\%}$ is the concentration of PFCA in condensate at 90% evaporation. $V_{C,\,90\%}$ is the volume of condensate at 90% evaporation.

As shown in Figure 10, almost all of PFCA remained in the leachate residual. The mass recovery of PFCA was more than 100% for all PFCA except for PFNA. This could be explained by reactions that could convert PFCA precursors to PFCA at the high temperature for evaporation.

Table 9 summarizes the distribution of PFCAs and PFOHs at 90% evaporation. Between 0.137% and 6.83% of PFCAs in mass was transferred to the condensate. The percentage of PFCAs mass in condensate increased with the increase of PFCA chain length. The only exception was PFDA. This could be explained by the fact that short-chain PFCAs have higher water solubility, making them to stay in the residual though shorter chain PFCAs have lower boiling points and higher vapor pressures (Wang et al., 2022; Xiao et al., 2023). FTOHs were almost completed transferred to the gas phase with less than 0.2% of FTOHs in condensate.

In control experiments, we evaporated the synthetic leachate, and took sample from the residual at 0% and 90% evaporation and the condensate at 90% evaporation. All 25 PFAS (measured by LC/MS/MS) were below the detection limit of 0.1 µg/L with the following exceptions: hexafluoropropylene oxide dimer acid (HFPO-DA) and PFNA was 0.820 µg/L and 0.400 µg/L, respectively in the synthetic leachate, and HFPO-DA, PFNA, and PFHpA were 5.300 µg/L, 0.300 µg/L, and 0.480 µg/L, respectively in the residual at 90% of evaporation. Therefore, the contamination was minor.

Table 8. Concentrations and removal percentages of PFCAs in the synthetic leachate

PFCA	Concentration (μg/L)			Removal percentage (%)	
	Residual at 0% evaporation	Residual at 90% evaporation	Condensate at 90% evaporation	Based on concentration[1]	Based on mass[2]
PFDA[3] (C10)	400	3,500	15.0	-775%	12.5%
PFNA[4] (C9)	420	5,600	37.0	-1,230%	-33.3%
PFOA[5] (C8)	500	6,100	23.0	-1,120%	-22.0%
PFHpA[6] (C7)	490	5,500	2.20	-1,020%	-12.24%
PFHxA[7] (C6)	440	5,300	1.20	-1,100%	-20.5%
PFPeA[8] (C5)	520	6,500	1.10	-1,150%	-25.0%
PFBA[9] (C4)	400	4,900	0.710	-1,130%	-22.5%

Notes:

[1] Removal percentage in leachate residual was calculated by (concentration in residual at 0% evaporation - concentration in residual at 90% evaporation)/ concentration in residual at 0% evaporation.

[2] Removal percentage in leachate residual based on mass was calculated by (concentration in residual at 0% evaporation × volume in residual at 0% evaporation - concentration in residual at 90% evaporation × concentration in residual at 90% evaporation)/ (concentration in residual at 0% evaporation × volume of residual at 0% evaporation).

[3] PFDA= Perfluorodecanoic acid

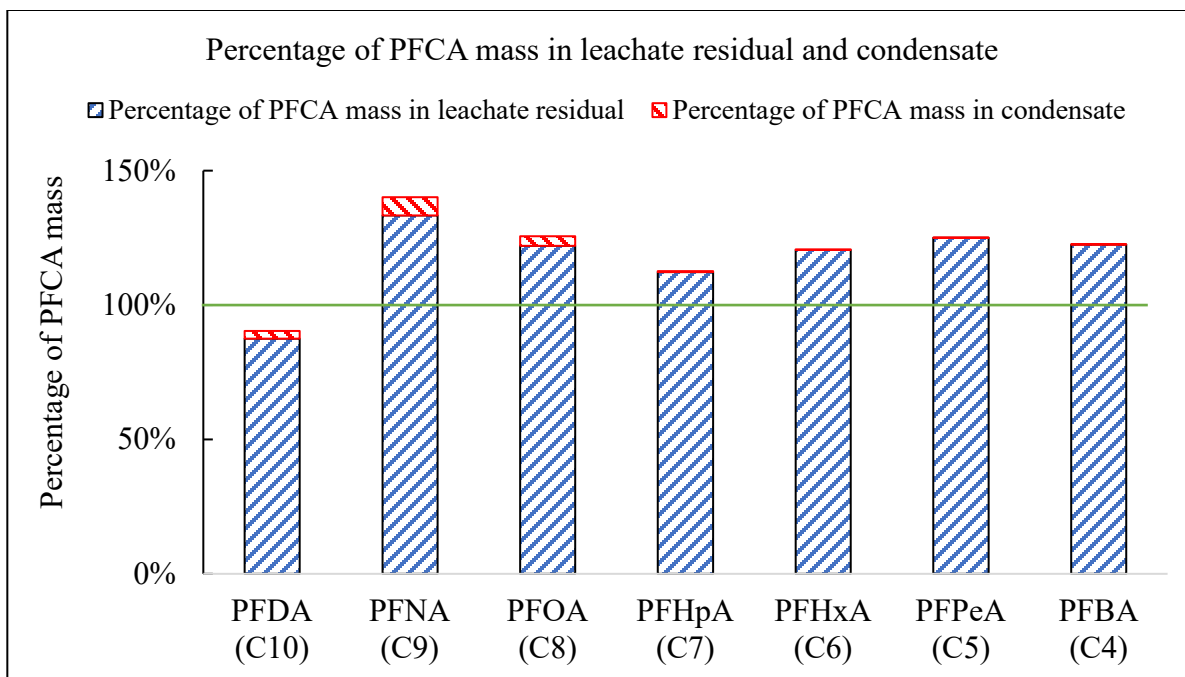[4] PFNA= Perfluorononanoic acid

[5] PFOA= Perfluorooctanoic acid

[6] PFHpA= Perfluoroheptanoic acid

[7] PFHxA= Perfluorohexanoic acid

[8] PFPeA= Perfluoropentanoic acid

[9] PFBA= Perfluorobutanoic acid

Figure 10. Percentage of PFCA mass in leachate residual and condensate at 90% evaporation compared to the initial PFCA mass in leachate

Table 9. Distribution ratios of PFCAs and FTOHs

Category	PFAS	Percentage of mass in residual (%)	Percentage of mass in condensate (%)	Percentage of mass in other (due to reaction or transfer to the gas phase) (%)
PFCAs[1]	PFDA[2] (C10)	87.5	2.91	9.59
	PFNA[3] (C9)	133	6.83	-39.8
	PFOA[4] (C8)	122	3.57	-25.6
	PFHpA[5] (C7)	112	0.348	-12.3
	PFHxA[6] (C6)	120	0.211	-20.2
	PFPeA[7] (C5)	125	0.164	-25.2
	PFBA[8] (C4)	123	0.138	-23.1
FTOHs[9]	10:2 FTOH[10]	0	0	100
	8:2 FTOH[11]	0	0.01	99.99
	6:2 FTOH[12]	0	0	100
	4:2 FTOH[13]	0	0.14	99.86

[1] PFCA= Perfluoroalkyl carboxylic acids
[2] PFDA= Perfluorodecanoic acid
[3] PFNA= Perfluorononanoic acid
[4] PFOA= Perfluorooctanoic acid
[5] PFHpA= Perfluoroheptanoic acid
[6] PFHxA= Perfluorohexanoic acid
[7] PFPeA= Perfluoropentanoic acid
[8] PFBA= Perfluorobutanoic acid
[9] FTOHs= Fluorotelomer alcohols
[10] 10:2 FTOH= 10:2 Fluorotelomer alcohol
[11] 8:2 FTOH= 8:2 Fluorotelomer alcohol
[12] 6:2 FTOH= 6:2 Fluorotelomer alcohol
[13] 4:2 FTOH= 4:2 Fluorotelomer alcohol

3.3. Effects of reintroduction of the concentrated leachate residuals (Task 3)

We evaporate the mixture that contained 160 mL leachate residual #1 at 90% evaporation and 1,440 mL leachate residual #1 at 0% evaporation. We took samples and measured various compounds in the 5 groups, including general physical parameters, general chemical parameters, metals, organic contaminants, and PFAS.

Category 1 -- general physical parameters: As shown in Figure 11, the TDS and TSS concentrations in the residual were more than two times higher for the mixture than for leachate #1, suggesting that the reintroduction of leachate residual led to accumulation of TDS and TSS. However, the introduction of the leachate residual did not change the quality of the condensate.
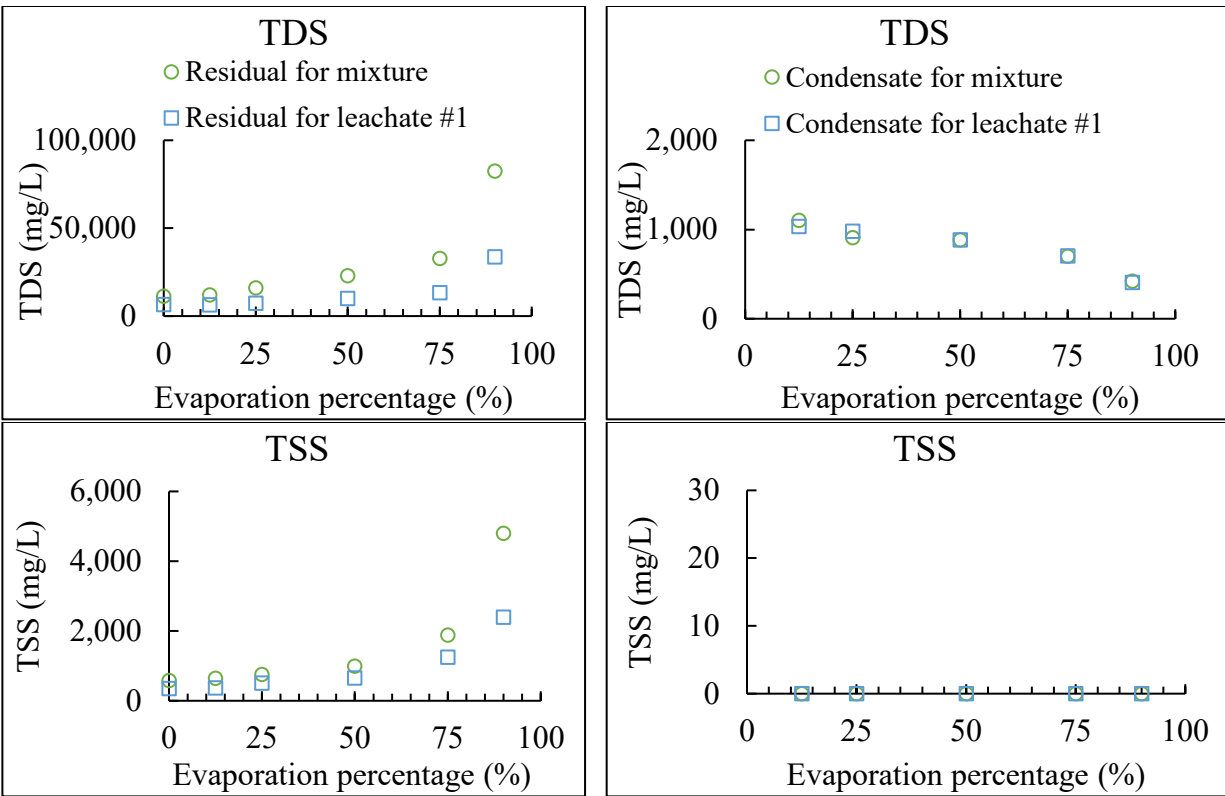
Figure 11. General physical parameters in the leachate residual (left) and condensate (right) for the mixture and leachate 1.

Category 2 -- general chemical parameters: As shown in Figure 12, the pH-related OH-, COD and BOD in the residual were less than 2 times higher for the mixture compared to leachate 1, suggesting that they also accumulated due to introduction for the concentrated leachate residual, but they accumulate less than TSS and TDS. On the contrary, the ammonia's concentration in the residual was smaller for the mixture than leachate 1 due to dilution by the concentrated residual. For all the parameters, the effects of the reintroduction of the concentrated leachate residual on the condensate was negligible.
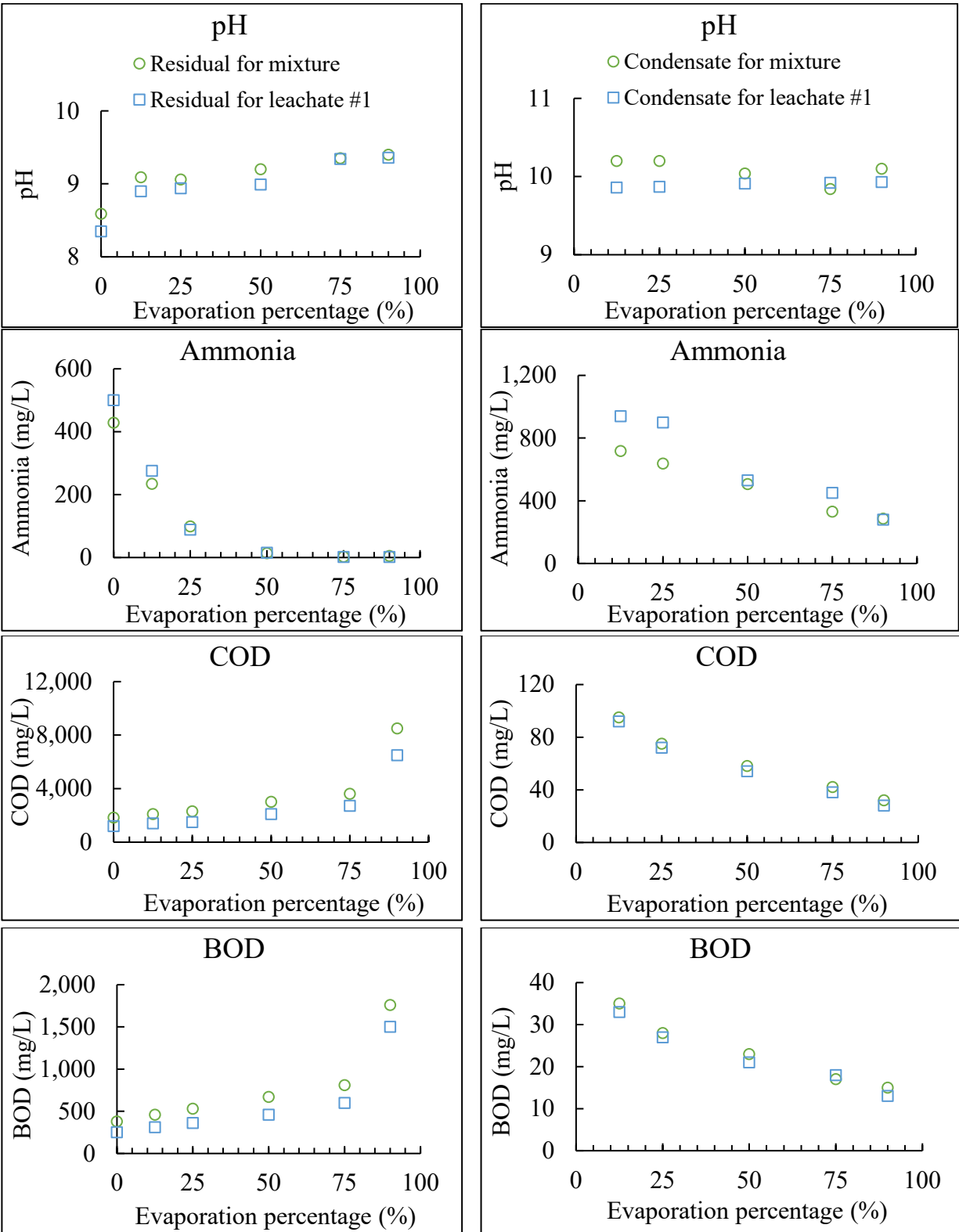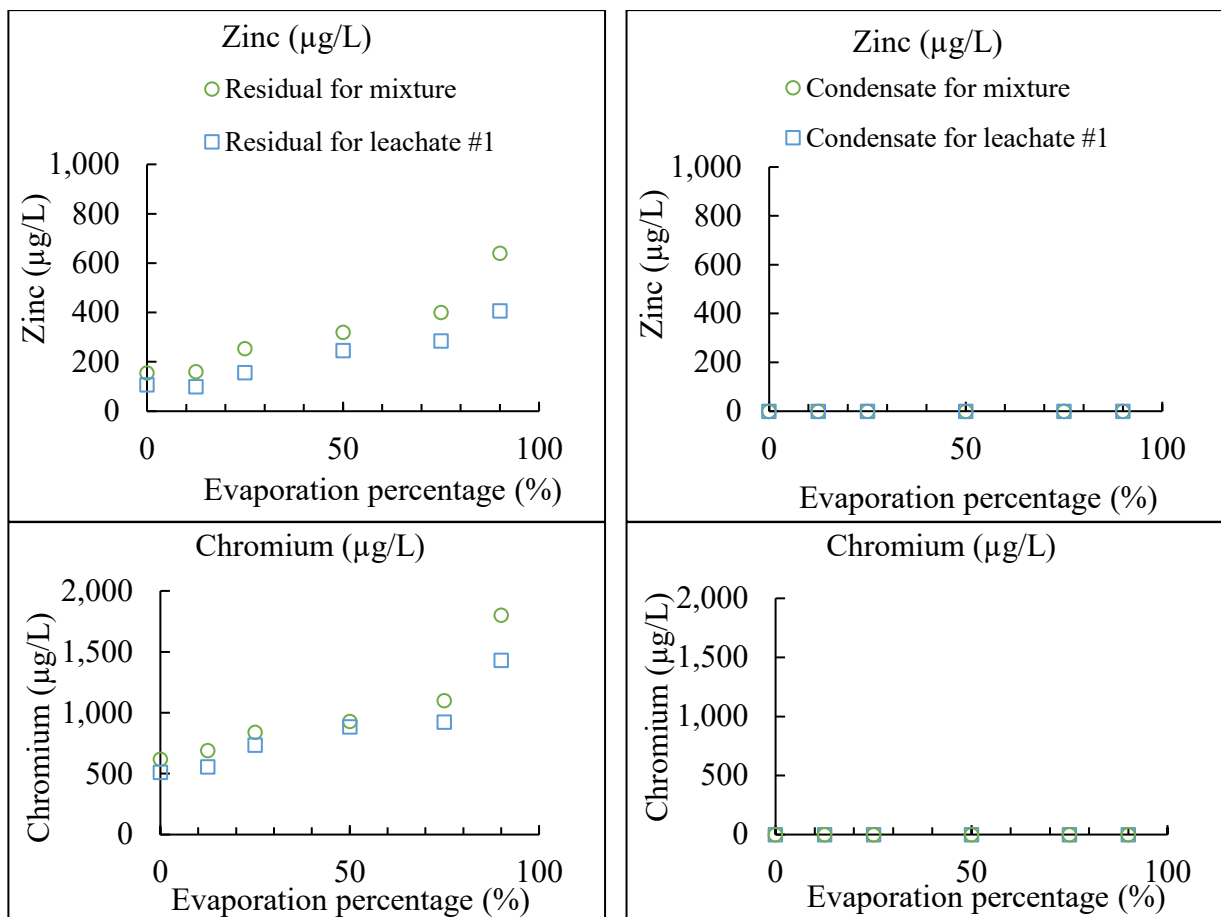
Figure 12. General chemical parameters in the leachate residual (left) and condensate (right) for the mixture and leachate 1.

Category 3 -- metals: As shown in Figure 13, zinc and chromium accumulated due to the reintroduction of the concentrated leachate residual.
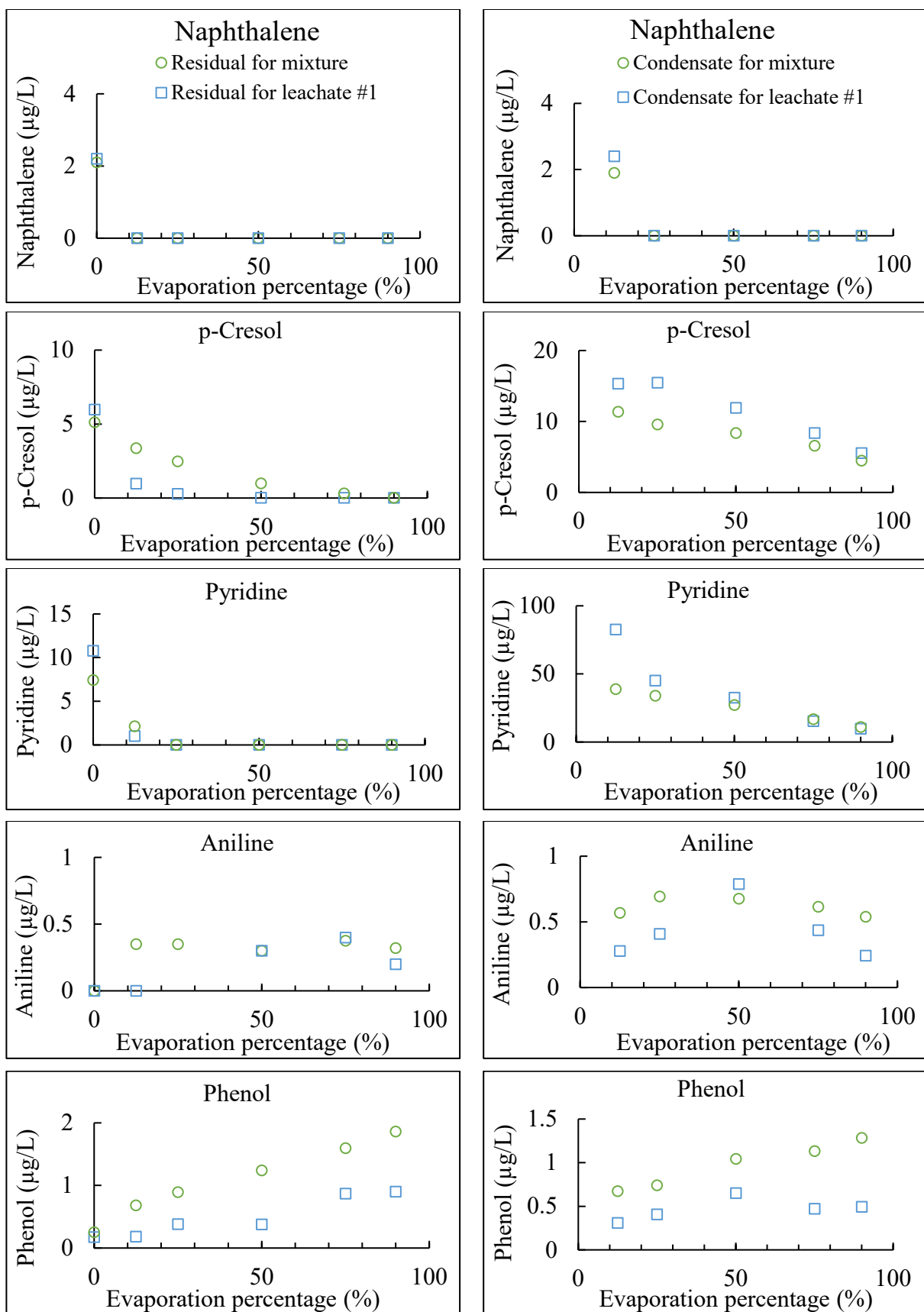

Figure 13. Metals in the leachate residual (left) and condensate (right) for the mixture and leachate 1. Arsenic was below the detection limit of 100 µg/L.

Category 4 -- organic compounds:
The concentrations for naphthalene, p-cresol, and pyridine in the residual were slightly lower for the mixture compared to leachate 1 (Figure 14). This can be explained by the fact that the concentrated leachate contained none or negligible levels of these volatile compounds; this diluted the mixture compared to leachate 1. On the other hand, the concentrations of aniline and phenol in the residual were higher for the mixture compared to leachate 1. This might be caused by the production of them via chemicals in the leachate and the concentrated residual.

Category 5 -- PFAS: The concentrations of 4:2 FTOH, 6:2 FTOH, 8:2 FTOH, 10:2 FTOH in all samples for the mixture were below the detection limit of 0.020 µg/L, 0.006 µg/L, 0.006 µg/L, and 0.020 µg/L, respectively.

Figure 14. Organic compounds in the leachate residual (left) and condensate (right) for the mixture and leachate 1

4. CONCLUSIONS

In this study, we used a rotary evaporator to evaluate the fate of contaminants in landfill leachate. The contaminants fell into five groups, including 1) general physical parameters, 2) general chemical parameters, 3) metals, 4) organic contaminants, and 5) PFAS. We evaporated landfill leachates sampled from three Florida landfills. We took samples from the leachate residual and condensate when 0%, 12.5%, 25%, 50%, 75%, and 90% evaporation was completed. TDS and TSS (in group 1) in leachate residuals increased continuously as evaporation continued. More than 50% of TDS and TSS in mass remained in the residual when 90% evaporation was achieved. TDS in the condensates at 90% evaporation were less than 2% of the TDS compared to its initial mass in the raw leachate before evaporation. No TSS was detected in the condensates. The rest (<50%) ended up in the gas-phase since part of TSS and TDS were volatile.

In group 2, the change patterns of TOC, COD, and BOD_5 for the three leachates were similar: They kept increasing in the leachate residuals due to accumulation and decreasing in the condensates due to dilution. At 90% evaporation, more than 50% of TOC, COD, and BOD_5 remained in the residuals except for BOD_5 in one leachate. The rest were transferred to the condensate and gas phase. Ammonia is semi-volatile. Its concentration steadily decreased in the leachate residuals and condensates. Mass balance shows that ammonia initially went to the condensates and then to the gas phase. Upon 90% of evaporation, 51-98% of ammonia in mass was removed from the system (i.e., residuals and condensates). The pattern of pH change depended on the leachate.

In group 3, zinc and chromium accumulated in leachate residual during the evaporation since their concentrations kept increasing in the residuals during evaporation. None of them were transferred to the condensate. At 90% of evaporation, 24-45% of these metals in mass stayed in the leachate residual, while the rest probably precipitated to the bottom of the evaporator and firmly attached to the bottom. This portion of metals was not measured as part of the residuals, but they likely belonged to the residuals.

In group 4, the concentration change patterns for naphthalene, p-cresol, and pyridine were similar to that for ammonia: Their concentrations steadily decreased in the residuals and condensates since all of them have high vapor pressures. The concentrations of naphthalene, p-cresol, and pyridine in the leachate residuals reached below their detection limits at 90% of evaporation. However, their fates varied: All naphthalene (100% in mass) were transferred to the gas phase; the majority of p-cresol (81-93% in mass) were transferred to the condensates; significant portions of pyridine were transferred to both the gas phase (21-53% in mass) and the condensates (47-79% in mass). The recovery for aniline and phenol were higher than 100% probably due to their production during the evaporation.

The PFAS in group 5 were divided into 4 PFAS measured by GC/MS (i.e., 4 FTOHs) and 25 PFAS measured by LC/MS/MS. Only one of the 4 FTOHs (6:2 FTOH) was detected above the limit at 0.021 µg/L in only one of the three leachates. It was removed from the system (i.e., residual and condensate) before 12.5% evaporation. Nine of the 25 PFAS measured by LC/MS/MS, including

6:2 fluorotelomer sulfonate (6:2 FTS), perfluoroheptane sulfonic acid (PFHpS), perfluorobutane sulfonic acid (PFBS), PFNA, PFOA, PFHpA, PFHxA, PFPeA, PFBA were above the detection limit of 0.22 µg/L and 0.1 µg/L in leachate #1 and leachate #2, respectively. Their removal percentages (based on mass) in the residuals varied between -18.4% and 23.9%. None of them were detected in the condensates, suggesting that they accumulated in leachate residuals.

To further evaluate the distribution of PFAS at 90% evaporation, we spiked a synthetic leachate with FTOHs and PFCAs (C4-C10) at 500 µg/L for each PFAS. More than 99.9% of each FTOH in mass were removed from the system (i.e., leachate residuals and condensates), with FTOHs below the detection limits in the residual and <0.2% in mass into the condensate. The concentrations of PFCAs in the leachate residual increased by 7.8 to 12 times at 90% evaporation, suggesting that they accumulated during the evaporation. Regarding distribution, 112-133% (in mass) of PFCAs except PFDA stayed in the leachate residual, 0.138%-6.83% (in mass) were transferred to the condensate, and -12.3 – -39.8% were produced due to reactions. More than 100% recovery in the residual was probably due to conversion from PFCA precursors during heating. We also found that the percentages of PFCAs (in mass) in condensate increased with the increase of PFCA chain length, probably due to lower solubility of longer-chain PFACs.

We mixed leachate #1 with its concentrated residual corresponding to 90% evaporation at a volume ratio of 9:1, and then compared this mixture with leachate #1 for the fate of contaminants during evaporation. Adding the concentrated leachate residual significantly increased the concentrations of non-volatile compounds in the residual. For example, adding just 10% concentrated leachate residual could at least double the TDS and TSS in the residual at 90% evaporation. On the other hand, for volatile compounds such as ammonia, naphthalene, p-cresol, pyridine, and FTOHs, the reintroduction of residual slightly decreased their concentrations in the residual at 90% evaporation because of dilution by the concentrated leachate that contained no or negligible volatile compounds.

References

Abusallout, I., Holton, C., Wang, J., & Hanigan, D. (2022). Henry's Law constants of 15 per-and polyfluoroalkyl substances determined by static headspace analysis. *Journal of Hazardous Materials Letters*, *3*, 100070.

Adeniyi, A., Bello, I., Mukaila, T., Monono, E., & Hammed, A. (2023). Developing rumen mimicry process for biological ammonia synthesis. *Bioprocess and Biosystems Engineering*, *46*(7), 1011-1020.

Aellab Labs, "ww.aellab.com", access in 2023

Afsharnia, M., Torabian, A., Mousavi, G. R., & Abduli, M. A. (2012). Landfill Leachate treatment by sono-evaporation. *Desalination and water Treatment*, *48*(1-3), 344-348.

American Public Health Association. "APHA standard methods for the examination of water and wastewater." *Standard methods for the examination of water & wastewater. Washington, DC: American Public Health Association* (2005).

Babaei, S., Sabour, M. R., & Moftakhari Anasori Movahed, S. (2021). Combined landfill leachate treatment methods: an overview. *Environmental Science and Pollution Research*, 1-14.

Baderna, D., Caloni, F., & Benfenati, E. (2019). Investigating landfill leachate toxicity in vitro: A review of cell models and endpoints. *Environment International*, *122*, 21-30.

Bakhshoodeh, R., Alavi, N., Oldham, C., Santos, R. M., Babaei, A. A., Vymazal, J., & Paydary, P. (2020). Constructed wetlands for landfill leachate treatment: A review. *Ecological Engineering*, *146*, 105725.

Birchler, D. R., Milke, M. W., Marks, A. L., & Luthy, R. G. (1994). Landfill leachate treatment by evaporation. *Journal of Environmental Engineering*, *120*(5), 1109-1131.

Bouchareb, R., Isik, Z., Ozay, Y., Karagunduz, A., Keskinler, B., & Dizge, N. (2022). A hybrid process for leachate wastewater treatment: Evaporation and reverse osmosis/sequencing batch reactor. *Water Environment Research*, *94*(4), e10717.

Çeçen, F., & Aktaş, Ö. (2004). Aerobic co-treatment of landfill leachate with domestic wastewater. *Environmental Engineering Science*, *21*(3), 303-312.

Cheng, S. Y., Show, P. L., Juan, J. C., Chang, J. S., Lau, B. F., Lai, S. H., ... & Ling, T. C. (2021). Landfill leachate wastewater treatment to facilitate resource recovery by a coagulation-flocculation process via hydrogen bond. *Chemosphere*, *262*, 127829.

Chian, E. S., & DeWalle, F. B. (1976). Sanitary landfill leachates and their treatment. *Journal of the Environmental Engineering Division*, *102*(2), 411-431.

Crownover, E., Oberle, D., Kluger, M., & Heron, G. (2019). Perfluoroalkyl and polyfluoroalkyl substances thermal desorption evaluation. *Remediation Journal*, *29*(4), 77-81.

Di Palma, L., Ferrantelli, P., Merli, C., & Petrucci, E. (2002). Treatment of industrial landfill leachate by means of evaporation and reverse osmosis. *Waste management*, *22*(8), 951-955.

ECFR, In Electronic Code of Federal Regulations. Retrieved 10, 17, 2023 from https://www.ecfr.gov/current/title-40/chapter-I/subchapter-N/part-445/subpart-A/section-445.11

Elnakar, H., & Buchanan, I. (2020). Soluble chemical oxygen demand removal from bypass wastewater using iron electrocoagulation. *Science of The Total Environment*, *706*, 136076.

Ferraz, F. M., & Yuan, Q. (2020a). Performance of oat hulls activated carbon for COD and color removal from landfill leachate. *Journal of Water Process Engineering*, *33*, 101040.

Ferraz, F. M., & Yuan, Q. (2020b). Organic matter removal from landfill leachate by adsorption using spent coffee grounds activated carbon. *Sustainable Materials and Technologies*, *23*, e00141.

Figoli, N. S., H. R. Keselman, P. C. L'Argentiere, and C. L. Lazzaroni. "Hydrolysis of chlorobenzene over Cu-promoted hydroxyapatites." *Journal of Catalysis* 77, no. 1 (1982): 64-73.

Keyikoglu, R., Karatas, O., Rezania, H., Kobya, M., Vatanpour, V., & Khataee, A. (2021). A review on treatment of membrane concentrates generated from landfill leachate treatment processes. *Separation and purification technology*, *259*, 118182.

Li, X., Rao, N. R. H., Linge, K. L., Joll, C. A., Khan, S., & Henderson, R. K. (2019). An evaluation of measurement techniques for algal-derived organic nitrogen. *Water research*, *165*, 114998.

Liang, L., Han, D., Ma, R., & Peng, T. (2013). Treatment of high-concentration wastewater using double-effect mechanical vapor recompression. *Desalination*, *314*, 139-146.

Liu, Z., Wu, W., Shi, P., Guo, J., & Cheng, J. (2015). Characterization of dissolved organic matter in landfill leachate during the combined treatment process of air stripping, Fenton, SBR and coagulation. *Waste Management*, *41*, 111-118.

Opio, A., Jones, M. B., Kansiime, F., & Otiti, T. (2015). Dissolved organic carbon in a tropical wetland dominated by Cyperus papyrus. *Wetlands ecology and management*, *23*, 1033-1038.

Rehman, Aziz-ur. "Landfill leachate treatment using evaporation technology." PhD diss., Carleton University, 2004

Reinhart, D. R., & Basel Al-Yousfi, A. (1996). The impact of leachate recirculation on municipal solid waste landfill operating characteristics. *Waste Management & Research*, *14*(4), 337-346.

Renou, S., Givaudan, J. G., Poulain, S., Dirassouyan, F., & Moulin, P. J. J. O. H. M. (2008). Landfill leachate treatment: Review and opportunity. *Journal of hazardous materials*, *150*(3), 468-493.

Ribera-Pi, J., Badia-Fabregat, M., Espí, J., Clarens, F., Jubany, I., & Martínez-Lladó, X. (2021). Decreasing environmental impact of landfill leachate treatment by MBR, RO and EDR hybrid treatment. *Environmental technology*, *42*(22), 3508-3522.

Rice, E. W., Bridgewater, L., & American Public Health Association (Eds.). (2012). *Standard methods for the examination of water and wastewater* (Vol. 10). Washington, DC: American public health association.

Sagandykova, G. N., Alimzhanova, M. B., Nurzhanova, Y. T., & Kenessov, B. (2017). Determination of semi-volatile additives in wines using SPME and GC–MS. *Food Chemistry*, *220*, 162-167.

Sanphoti, N., Towprayoon, S., Chaiprasert, P., & Nopharatana, A. (2006). The effects of leachate recirculation with supplemental water addition on methane production and waste

decomposition in a simulated tropical landfill. *Journal of Environmental Management*, *81*(1), 27-35.

Schiopu, A. M., & Gavrilescu, M. (2010). Options for the treatment and management of municipal landfill leachate: common and specific issues. *CLEAN–Soil, Air, Water*, *38*(12), 1101-1110.

Simões, N. G., Cardoso, V. V., Ferreira, E., Benoliel, M. J., & Almeida, C. M. (2007). Experimental and statistical validation of SPME-GC–MS analysis of phenol and chlorophenols in raw and treated water. *Chemosphere*, *68*(3), 501-510.

Sprovieri, J. A. S., de Souza, T. S. O., & Contrera, R. C. (2020). Ammonia removal and recovery from municipal landfill leachates by heating. *Journal of environmental management*, *256*, 109947 https://doi.org/10.1016/j.jenvman.2019.109947

Stull, D. R. (1947). Vapor pressure of pure substances. Organic and inorganic compounds. *Industrial & Engineering Chemistry*, *39*(4), 517-540.

Suárez García, E., & CARDONA-GALLO, S. A. (2013). Nitrogen removal from landfill leachate using a sequential biological passive system. Dyna, 80(178), 37-43.

Taniguchi, T., Imoto, M., Takeda, M., Nakai, T., Mihara, M., Iwai, T., ... & Ogawa, A. (2015). Hydrolysis of Diazonium Salts Using a Two-Phase System (CPME and Water). *Heteroatom Chemistry*, *26*(6), 411-416.

Tang, Y., Goukeh, M.N., Eeso, K., 2023. Per- and Polyfluoroalkyl Substances (PFAS) in Landfill Gas Emissions

Teng, C., Zhou, K., Peng, C., & Chen, W. (2021). Characterization and treatment of landfill leachate: A review. *Water research*, *203*, 117525.

Wang, J., Lin, Z., He, X., Song, M., Westerhoff, P., Doudrick, K., & Hanigan, D. (2022). Critical review of thermal decomposition of per-and polyfluoroalkyl substances: mechanisms and implications for thermal treatment processes. *Environmental Science & Technology*, *56*(9), 5355-5370.

Wiszniowski, J., Robert, D., Surmacz-Gorska, J., Miksch, K., & Weber, J. V. (2006). Landfill leachate treatment methods: A review. *Environmental chemistry letters*, *4*, 51-61.

Xiao, F., Challa Sasi, P., Alinezhad, A., Sun, R., & Abdulmalik Ali, M. (2023). Thermal phase transition and rapid degradation of forever chemicals (PFAS) in spent media using induction heating. *ACS ES&T Engineering*.

Zarębska, M., & Bajkacz, S. (2023). Poly–and perfluoroalkyl substances (PFAS)-recent advances in the aquatic environment analysis. *TrAC Trends in Analytical Chemistry*, 117062.

Zhang, Q., Guo, M., Xie, J., Yang, X., & Chen, C. (2022). Investigation on characteristics of landfill leachate and feasibility study of low-temperature vacuum evaporation treatment. *Journal of Environmental Chemical Engineering*, *10*(5), 108451.

Zhou, Y., Shi, C., & Dong, G. (2014). Analysis of a mechanical vapor recompression wastewater distillation system. *Desalination*, *353*, 91-97.
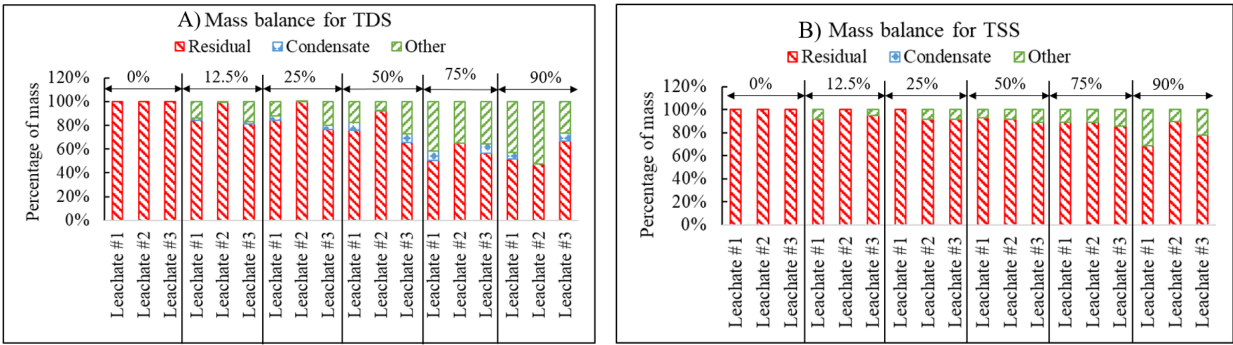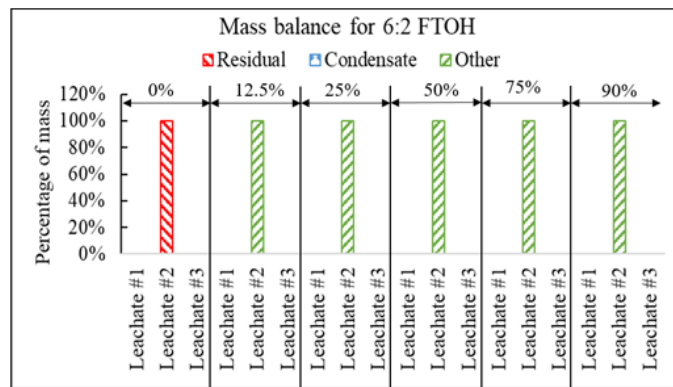
Figure A1. Mass balance for A) TDS and B) TSS during leachate evaporation
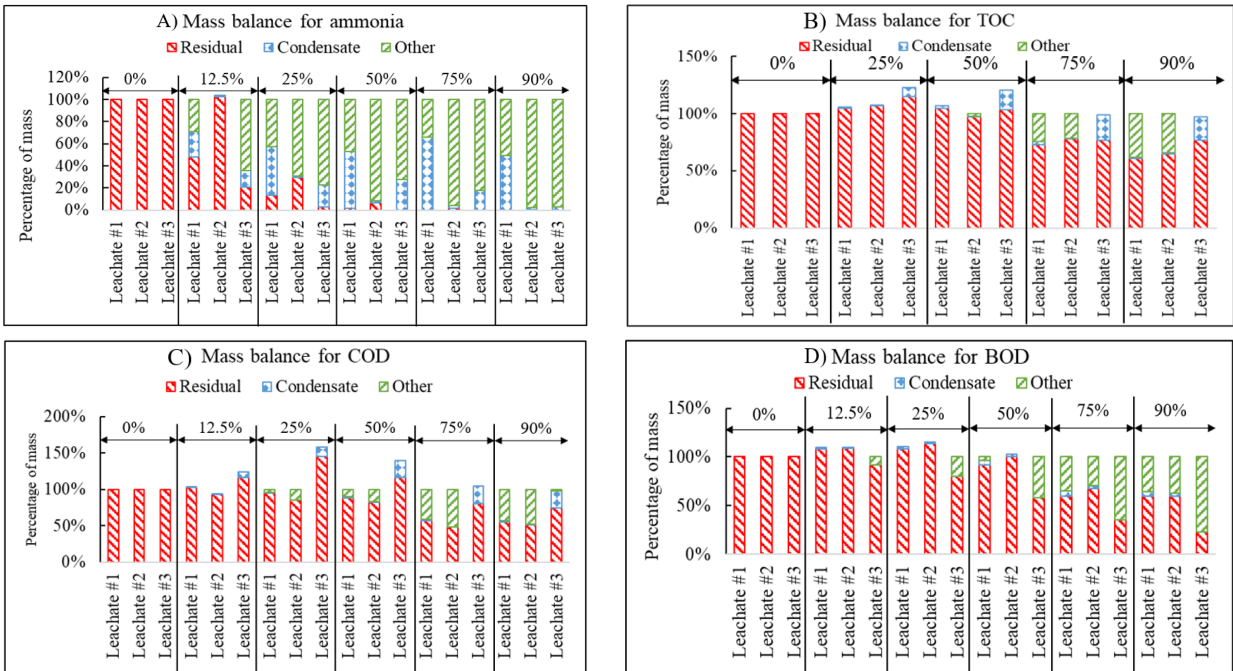
Figure A2. Mass balance for A) ammonia, B) TOC, C) COD, and D) BOD during leachate evaporation

Figure A3. Mass balance for A) zinc and B) chromium during leachate evaporation

Figure A4. Mass balance for A) naphthalene, B) p-cresol, C) pyridine, D) aniline, and E) phenol during leachate evaporation.

Figure A5. Mass balance for 6:2 FTOH